

Nonlinear multi-study factor analysis

Gemma Moran*

Department of Statistics, Rutgers University

and

Anandi Krishnan

Department of Biomedical Engineering, Rutgers University

January 27, 2026

Abstract

High-dimensional data often exhibit variation that can be captured by lower dimensional factors. For high-dimensional data from multiple studies or environments, one goal is to understand which underlying factors are common to all studies, and which factors are study or environment-specific. As a particular example, we consider platelet gene expression data from patients in different disease groups. In this data, factors correspond to clusters of genes which are co-expressed; we may expect some clusters (or biological pathways) to be active for all diseases, while some clusters are only active for a specific disease. To learn these factors, we consider a nonlinear multi-study factor model, which allows for both shared and specific factors. To fit this model, we propose a multi-study sparse variational autoencoder. The underlying model is sparse in that each observed feature (i.e. each dimension of the data) depends on a small subset of the latent factors. In the genomics example, this means each gene is active in only a few biological processes. Further, the model implicitly induces a penalty on the number of latent factors, which helps separate the shared factors from the group-specific factors. We prove that the latent factors are identified, and demonstrate our method recovers meaningful factors in the platelet gene expression data.

Keywords: *nonlinear dimensionality reduction, unsupervised learning, multiple environments*

*The authors gratefully acknowledge Rutgers Cyberinfrastructure and AI for Science and Society, and NIH Grant 1R21HL181649

1 Introduction

In many domains, high-dimensional data have a much smaller intrinsic dimensionality. A common goal is to reduce such high-dimensional data to lower-dimensional latent factors. These latent factors summarize the variability inherent in the observed data.

Often, instead of a single high-dimensional dataset, we observe multiple datasets from different studies or environments. A key question with such data is: what factors are shared across studies, and what factors are study-specific? In genomics, for example, it is common to collect gene expression measurements from patients from different hospitals, or with different conditions.

As a particular example, we study gene expression levels in blood platelets from patients with diverse diseases. Platelets serve as a “circulating biosensor” that captures information from parent megakaryocytes and the bone marrow microenvironment, as well as systemic signals including inflammation, immune activation, and drug effects ([Krishnan and Best, 2025](#); [Thomas et al., 2024](#); [Rowley et al., 2019](#); [Weyrich, 2014](#)). Notably, platelet transcriptomes exhibit both conserved molecular pathways active across disease states and disease-specific pathway dysregulation. By investigating which genes are co-expressed within and across disease categories - particularly comparing cardiovascular, immune-mediated, cancer, and hematologic diseases - we can identify shared biomarkers and therapeutic targets, as well as understand disease-specific platelet dysfunction mechanisms.

In the statistics literature, recent work on this problem include multi-study factor analysis ([De Vito et al., 2019](#), MSFA) and subspace factor analysis ([Chandra et al., 2025](#), SUFA). In MSFA, a linear factor model is introduced with a common loadings matrix shared across studies, and study-specific loadings matrices. [Chandra et al. \(2025\)](#) propose an alternative parameterization of this model to identify the shared loadings from the study-specific loadings.

In the machine learning literature, there have been recent work modeling multi-study data using autoencoding frameworks. In these autoencoding models, the data is “encoded” into a low-dimensional representation space using a neural network. This low-dimensional representation is then “decoded” back to the original data space, again using a neural network. By jointly training the encoder and the decoder neural networks, the low-dimensional representation is encouraged to capture the important information in the original data. This autoencoding paradigm has been extended to multi-study data, primarily by modifying the decoder neural network into shared and study-specific components, combined with regularization ([Davison et al., 2019](#); [Weinberger et al., 2022](#)).

Both the statistical and machine learning approaches to this problem have advantages and disadvantages. The advantages of the statistical approach to multi-study factor

analysis are (i) interpretability; (ii) identifiability guarantees and (iii) principled uncertainty quantification, especially for Bayesian methods. However, a disadvantage of the statistical approach is the lack of flexibility; only linear models are considered. Meanwhile, the ML approaches allow for flexible function estimation via neural networks, but lack guarantees regarding identifiability, and are often not directly interpretable.

In this paper, we introduce a new method for multi-study factor analysis. In particular, we propose a nonlinear multi-study factor model which we fit using a sparse variational autoencoder (VAE). First, the model is flexible in that we use neural networks to learn the shared and study-specific latent factors. Second, the model is interpretable in that we can inspect which features (dimensions of the data) depend on which latent factor dimensions; this allows us to interpret the factors in a similar way to sparse linear factor analysis. Third, we prove that we can identify the shared factors from the study-specific factors.

Overview. In § 1.1 we provide a more thorough literature review of the statistical and machine learning approaches to the multi-study problem. In § 2.2 we introduce our method, multi-study sparse variational autoencoder (MSSVAE). In § 3 we prove identifiability for the single-study model and extend to the multi-study model. In § 4, we demonstrate the performance of the MSSVAE on a variety of synthetic datasets. In § 5, we analyze the real platelet gene expression data.

1.1 Related Work

Linear methods. There are a number of recent works which propose linear factor models for the multi-study setting. [De Vito et al. \(2019\)](#) introduced the multi-study factor analysis (MSFA) model, a linear factor analysis model with a shared loadings matrix across all studies, and study-specific loadings matrices. [De Vito et al. \(2021\)](#) extended this MSFA model to high-dimensional data, including sparsity-inducing priors on the loading matrices and fit with an MCMC algorithm. Instead of MCMC, [Hansen et al. \(2025\)](#) introduced faster variational inference algorithms for the MSFA model. [Jerby-Arnon et al. \(2021\)](#) also consider a linear matrix decomposition with shared and study-specific loadings matrices, fit with a regularized optimization scheme.

[Chandra et al. \(2025\)](#) highlight that linear multi-study factor models can have an identifiability problem; specifically, the solution where the shared factors are zero and the study-specific factors have all the signal is observationally indistinguishable from the model which correctly separates shared and study specific factors. To fix this identifiability problem, they propose an alternative linear parameterization.

[Sturma et al. \(2023\)](#) consider the linear multi-study setting where the latent factors now have an unknown dependence structure. They posit a linear model with shared and study-specific

latent factors, introduce a algorithm to first identify shared variation across studies, and then learn a causal graph over the shared latent factors. For this model and algorithm, [Sturma et al. \(2023\)](#) prove that the resultant factors are identified.

Finally, [Grabski et al. \(2023\)](#) study a linear multi-study factor model where factors can be shared across a subset of the studies (instead of all the studies); these subsets are learned jointly with the latent factors.

Nonlinear methods. Nonlinear approaches to the multi-study setting have also been recently proposed. [Davison et al. \(2019\)](#) propose a the Cross-Population Variational Autoencoder, an autoencoding model where the decoding function is a linear combination of a nonlinear function of the shared factors with separate nonlinear functions of the specific factors. In contrast, our approach uses a nonlinear decoder.

[Weinberger et al. \(2022\)](#) propose a more flexible model called multiGroupVI. The multi-GroupVI model consists of both shared encoders and study-specific encoders which learn latent shared factors and study-specific factors, respectively. To map the latent factors back to the data space, multiGroupVI uses a single decoder for both the shared and study-specific factors. The multiGroupVI method is not directly interpretable in terms of which features (e.g. genes) are associated with shared or study-specific factors. To find study-specific genes, [Weinberger et al. \(2022\)](#) see which genes have the largest Bayes factors when comparing the whole model to a shared factor-only model. In contrast, our approach is inherently interpretable due to the sparsity in our decoder.

2 Methods

2.1 Review: Multi-study linear factor analysis

The observed data is $\mathbf{X}^{(m)} \in \mathbb{R}^{n_m \times G}$, where n_m is the number of samples from study m and G is the number of observed features (e.g. genes). That is, for each study $m = 1, \dots, M$, we observe the same set of features.

We first review the linear multi-study factor analysis (MSFA) model of [De Vito et al. \(2019\)](#). The MSFA model is:

$$\mathbf{x}_i^{(m)} = \Phi \mathbf{z}_i^{(m)} + \Lambda^{(m)} \zeta_i^{(m)} + \boldsymbol{\varepsilon}_i^{(m)}, \quad \boldsymbol{\varepsilon}_i^{(m)} \stackrel{iid}{\sim} N(0, \Sigma^{(m)}),$$

where $\Phi \in \mathbb{R}^{G \times K_S}$ is the latent loadings matrix shared across studies, $\mathbf{z}_i^{(m)} \in \mathbb{R}^{K_S}$ are the latent factors in the shared subspace, $\Lambda^{(m)} \in \mathbb{R}^{G \times K_m}$ is the m th study specific latent loadings matrix and $\zeta_i^{(m)}$ the corresponding latent factors. The noise vector $\boldsymbol{\varepsilon}$ has study-specific diagonal covariance $\Sigma^{(m)} = \text{diag}\{\sigma_1^{(m)}, \dots, \sigma_G^{(m)}\}$. Note that the data is not paired (i.e. $\mathbf{x}_i^{(m)}$ and $\mathbf{x}_i^{(m')}$ are data from different samples).

For the MSFA model, the marginal covariance of the data is:

$$\text{Cov}(\mathbf{x}_i^{(m)}) = \boldsymbol{\Phi}\boldsymbol{\Phi}^\top + \boldsymbol{\Lambda}^{(m)}\boldsymbol{\Lambda}^{(m)\top} + \boldsymbol{\Sigma}^{(m)}. \quad (2.1)$$

For each column $\boldsymbol{\Phi}_{\cdot k} \in \mathbb{R}^G$, the genes with nonzero values can be interpreted as cluster. Genes within a cluster have correlated expression levels across all studies. Such gene clusters may be useful for developing hypotheses about biological processes which are shared across studies. (Note that genes can belong to more than one cluster.) Similarly, $\boldsymbol{\Lambda}_{\cdot k'}^{(m)} \in \mathbb{R}^G$ corresponds to gene clusters that are only present in the m th study. In the next section, we extend the MSFA model to the nonlinear case while retaining this interpretability from the shared and study-specific loadings matrices.

2.2 Multi-study sparse deep generative model

To allow for nonlinear relationships between the data and the latent factors, we propose a sparse deep generative model (DGM) for multi-study data. To retain the interpretability of a linear model, we introduce a sparse masking parameter which allows the observed feature to depend on a subset of the latent factors. Our proposal is an extension of the sparse deep generative model of [Moran et al. \(2022\)](#) to the multi-study setting.

More specifically, our sparse DGM for multi-study data is: for $i = 1, \dots, n_m$ and $j = 1, \dots, G$,

$$x_{ij}^{(m)} = f_{\theta, j}(\tilde{\mathbf{w}}_j^{(m)} \odot \tilde{\mathbf{z}}_i^{(m)}) + \varepsilon_{ij}^{(m)}, \text{ where } \varepsilon_{ij}^{(m)} \stackrel{iid}{\sim} \mathcal{N}(0, \sigma_j^2), \quad (2.2)$$

where $f_\theta : \mathbb{R}^K \rightarrow \mathbb{R}^G$ is a feedforward neural network parameterized by θ . Above, we define $f_{\theta, j}(\mathbf{z}) := (f_\theta(\mathbf{z}))_j$ i.e. the j th element of f_θ . Further, σ_j^2 is noise variance for feature j , and \odot denotes the element-wise product. The sparse-per-feature vector $\tilde{\mathbf{w}}_j^{(m)} \in \mathbb{R}^K$ selects which latent factors are used to produce feature j in study m . The vector $\tilde{\mathbf{w}}_j^{(m)}$ combines shared and study-specific factor dimensions as:

$$\tilde{\mathbf{w}}_j^{(m)} = \left(\mathbf{w}_j^{(S)} \quad \mathbf{0}_{1 \times K_1} \quad \cdots \quad \mathbf{0}_{1 \times K_{m-1}} \quad \mathbf{w}_j^{(m)} \quad \mathbf{0}_{1 \times K_{m+1}} \quad \cdots \quad \mathbf{0}_{1 \times K_M} \right)^\top,$$

where $\mathbf{w}_j^{(S)}$ is shared across all studies, so that all studies select the same dimensions of the shared factor space to produce feature j . The vector $\mathbf{w}_j^{(m)}$ allows study m to additionally use study-specific latent factor dimensions to produce feature j . See [Figure 1](#) for an illustration. The zero padding in $\tilde{\mathbf{w}}_j$ is included because we use the same f_θ for all studies and so require the input of f_θ to be partitioned into shared and study-specific dimensions.

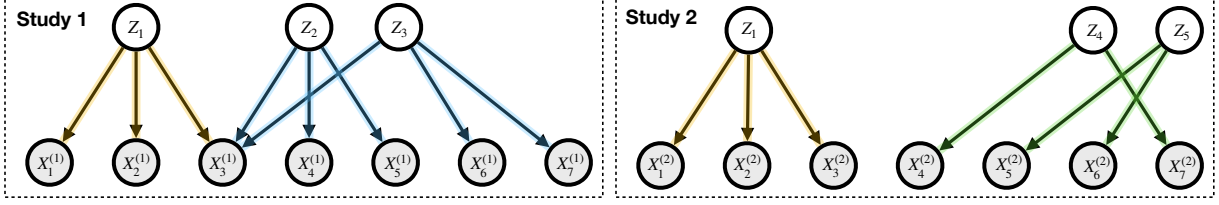


Figure 1: Example of a two-study sparse model: both study 1 and 2 share factor z_1 , whereas factors z_2, z_3 are specific to study 1, and factors z_4, z_5 are specific to study 2.

Similarly, the latent factors $\tilde{z}_i^{(m)}$ combine shared and study-specific dimensions:

$$\tilde{z}_i^{(m)} = (\mathbf{z}_i^{(m)} \quad \mathbf{0}_{1 \times K_1} \quad \cdots \quad \mathbf{0}_{1 \times K_{m-1}} \quad \boldsymbol{\zeta}_i^{(m)} \quad \mathbf{0}_{1 \times K_{m+1}} \quad \cdots \quad \mathbf{0}_{1 \times K_M})^\top,$$

where $\mathbf{z}_i^{(m)} \in \mathbb{R}^{K_S}$ are factors from the shared space and $\boldsymbol{\zeta}_i^{(m)} \in \mathbb{R}^{K_m}$ are factors from the study-specific space. Note that $\mathbf{z}_i^{(m)}$ are local variables specific to each sample i ; these factors are “shared” in that modulating $\mathbf{z}_i^{(m)}$ for any m will have the same effect on $\mathbf{x}_i^{(m)}$ (via the shared $\mathbf{w}^{(S)}$).

For all studies $m = 1, \dots, M$, the shared and study-specific factors are assigned standard normal priors:

$$\mathbf{z}_i^{(m)} \sim \mathcal{N}_{K_S}(\mathbf{0}, \mathbf{I}), \quad \boldsymbol{\zeta}_i^{(m)} \sim \mathcal{N}_{K_m}(\mathbf{0}, \mathbf{I}).$$

The error variances σ_j^2 are assigned inverse-gamma priors:

$$\sigma_j^2 \sim \text{Inverse-Gamma}(\nu/2, \nu\xi/2).$$

Similarly to [Moran et al. \(2022\)](#), the shared masking variables are assigned a sparsity-inducing prior, the spike-and-slab lasso ([Ročková and George, 2018](#)). Specifically, for $j = 1, \dots, G; k = 1, \dots, K_S$:

$$\begin{aligned} p(w_{jk}^{(S)} | \gamma_{jk}^{(S)}) &= \gamma_{jk}^{(S)} \frac{\lambda_1}{2} \exp(-\lambda_1 |w_{jk}^{(S)}|) + (1 - \gamma_{jk}^{(S)}) \frac{\lambda_0}{2} \exp(-\lambda_0 |w_{jk}^{(S)}|), \\ \gamma_{jk}^{(S)} | \eta_k^{(S)} &\sim \text{Bernoulli}(\eta_k^{(S)}), \\ \eta_k^{(S)} &\sim \text{Beta}(a_S, b_S). \end{aligned}$$

That is, *a priori* $w_{jk}^{(S)}$ is drawn from a Laplacian “slab” with parameter λ_1 , or a Laplacian “spike” with parameter λ_0 , where $\lambda_0 \gg \lambda_1$. The binary variable $\gamma_{jk}^{(S)} \in \{0, 1\}$ indicates whether $w_{jk}^{(S)}$ is drawn from the spike or slab; to allow for uncertainty over this draw, $\gamma_{jk}^{(S)}$ is assigned a Bernoulli distribution with parameter $\eta_k^{(S)}$. The parameter $\eta_k^{(S)}$ reflects the proportion of $w_{jk}^{(S)}$ drawn from the slab; different columns k are allowed to have different

proportions. The parameter $\eta_k^{(S)}$ itself is assigned a Beta prior with hyperparameters $a_S, b_S \in \mathbb{R}^+$. The hyperparameters a_S, b_S control the sparsity of $\gamma_{jk}^{(S)}$.

Notice the prior on $\eta_k^{(S)}$ helps to “zero out” extraneous factor dimensions and consequently estimate the number of factors K_S . If the hyperparameters are set to $a_S \propto 1/K$ and $b_S = 1$, the Beta-Bernoulli prior corresponds to the finite Indian Buffet Process prior (Griffiths and Ghahramani, 2005).

For the study-specific masking variables $w_{jk}^{(m)}$, we similarly assign spike-and-slab lasso priors (Ročková and George, 2018) with associated hyperpriors for $\gamma_{jk}^{(m)}, \eta_k^{(m)}$ and hyperparameters a_m, b_m . Finally, we denote $\mathbf{W}^{(S)} = [\mathbf{w}_1^{(S)} \cdots \mathbf{w}_G^{(S)}]^T$, $\boldsymbol{\Gamma}^{(S)} = (\gamma_{jk}^{(S)})_{1 \leq j \leq G, 1 \leq k \leq K}$ (similarly for $\mathbf{W}^{(m)}$ and $\boldsymbol{\Gamma}^{(m)}$).

2.3 Estimation

Similarly to Moran et al. (2022), we use approximate maximum *a posteriori* (MAP) estimation for the parameters $\{\theta, \mathbf{W}^{(S)}, \boldsymbol{\eta}^{(S)}, \{\mathbf{W}^{(m)}, \boldsymbol{\eta}^{(m)}\}_{m=1}^M, \boldsymbol{\Sigma}\}$ and amortized variational inference for the factors $\{\mathbf{z}_{1:n_m}^{(m)}, \boldsymbol{\zeta}_{1:n_m}^{(m)}\}_{m=1}^M$. This procedure for approximating the posterior is called a multi-study sparse VAE (MSSVAE).

The exact MAP objective (up to constant terms) is:

$$\begin{aligned} \log p_\theta & \left(\mathbf{W}^{(S)}, \boldsymbol{\eta}^{(S)}, \left\{ \mathbf{W}^{(m)}, \boldsymbol{\eta}^{(m)} \right\}_{m=1}^M, \boldsymbol{\Sigma} \middle| \{\mathbf{X}^{(m)}\}_{m=1}^M \right) \\ &= \sum_{m=1}^M \sum_{i=1}^{n_m} \log \left[\int p_\theta(\mathbf{x}_i^{(m)} | \mathbf{W}^{(S)}, \mathbf{W}^{(m)}, \mathbf{z}_i^{(m)}, \boldsymbol{\zeta}_i^{(m)}, \boldsymbol{\Sigma}) p(\mathbf{z}_i^{(m)}) p(\boldsymbol{\zeta}_i^{(m)}) d\mathbf{z}_i^{(m)} d\boldsymbol{\zeta}_i^{(m)} \right] \\ &+ \log p(\boldsymbol{\Sigma}) + \log \left[\int p(\mathbf{W}^{(S)} | \boldsymbol{\Gamma}^{(S)}) p(\boldsymbol{\Gamma}^{(S)} | \boldsymbol{\eta}^{(S)}) p(\boldsymbol{\eta}^{(S)}) d\boldsymbol{\Gamma}^{(S)} \right] \\ &+ \sum_{m=1}^M \log \left[\int p(\mathbf{W}^{(m)} | \boldsymbol{\Gamma}^{(m)}) p(\boldsymbol{\Gamma}^{(m)} | \boldsymbol{\eta}^{(m)}) p(\boldsymbol{\eta}^{(m)}) d\boldsymbol{\Gamma}^{(m)} \right]. \end{aligned} \quad (2.3)$$

The exact MAP objective is intractable; we lower bound the first term of Eq. 2.3 using variational inference. Specifically, for the shared dimensions $\mathbf{z}_{1:n_m}^{(m)}$, we use the variational family:

$$q_{\psi_S}(\mathbf{z}_i^{(m)} | \mathbf{x}_i^{(m)}) = N(\mu_{\psi_S}(\mathbf{x}_i^{(m)}), \text{diag}(\sigma_{\psi_S}^2(\mathbf{x}_i^{(m)})))$$

where $\mu_{\psi_S}, \sigma_{\psi_S}^2 : \mathbb{R}^{K_S} \rightarrow \mathbb{R}^G$ are neural networks parameterized by ψ_S . For the study-specific dimensions, $\boldsymbol{\zeta}_i^{(m)}$, we use a separate variational family for each study:

$$q_{\psi_m}(\boldsymbol{\zeta}_i^{(m)} | \mathbf{x}_i^{(m)}) = N(\mu_{\psi_m}(\mathbf{x}_i^{(m)}), \text{diag}(\sigma_{\psi_m}^2(\mathbf{x}_i^{(m)})))$$

where again $\mu_{\psi_m}, \sigma_{\psi_m}^2 : \mathbb{R}^{K_m} \rightarrow \mathbb{R}^G$ are neural networks parameterized by ψ_m .

Next, we lower bound the last two terms of the MAP objective (Eq. 2.3), again using variational inference:

$$\begin{aligned} q(\boldsymbol{\Gamma}^{(S)}) &= p(\boldsymbol{\Gamma}^{(S)} | \mathbf{W}_{\text{old}}^{(S)}, \boldsymbol{\eta}_{\text{old}}^{(S)}), \\ q(\boldsymbol{\Gamma}^{(m)}) &= p(\boldsymbol{\Gamma}^{(m)} | \mathbf{W}_{\text{old}}^{(m)}, \boldsymbol{\eta}_{\text{old}}^{(m)}), \quad m = 1, \dots, M, \end{aligned}$$

where $\{\mathbf{W}_{\text{old}}^{(\cdot)}, \boldsymbol{\eta}_{\text{old}}^{(\cdot)}\}$ denote the updates from the previous iteration of the algorithm. This choice corresponds to the usual expectation in the EM algorithm.

Bringing together these approximations, the MAP objective (Eq. 2.3) has the lower bound:

$$\begin{aligned} \mathcal{L}(\Theta) &= \sum_{m=1}^M \left\{ \sum_{i=1}^{n_m} \left\{ \mathbb{E}_{q_{\psi_S}(\mathbf{z}_i^{(m)} | \mathbf{x}_i^{(m)}) q_{\psi_m}(\boldsymbol{\zeta}_i^{(m)} | \mathbf{x}_i^{(m)})} \left[\log p_{\theta}(\mathbf{x}_i^{(m)} | \mathbf{W}^{(S)}, \mathbf{W}^{(m)}, \mathbf{z}_i^{(m)}, \boldsymbol{\zeta}_i^{(m)}, \boldsymbol{\Sigma}) \right] \right. \right. \\ &\quad \left. \left. - D_{KL}(q_{\psi_S}(\mathbf{z}_i^{(m)} | \mathbf{x}_i^{(m)}) || p(\mathbf{z}_i^{(m)})) - D_{KL}(q_{\psi_m}(\boldsymbol{\zeta}_i^{(m)} | \mathbf{x}_i^{(m)}) || p(\boldsymbol{\zeta}_i^{(m)})) \right\} \right. \\ &\quad \left. + \mathbb{E}_{\boldsymbol{\Gamma}^{(m)} | \mathbf{W}^{(m)}, \boldsymbol{\eta}^{(m)}} [\log p(\mathbf{W}^{(m)} | \boldsymbol{\Gamma}^{(m)}) p(\boldsymbol{\Gamma}^{(m)} | \boldsymbol{\eta}^{(m)}) p(\boldsymbol{\eta}^{(m)})] \right\} \\ &\quad \left. + \mathbb{E}_{\boldsymbol{\Gamma}^{(S)} | \mathbf{W}^{(S)}, \boldsymbol{\eta}^{(S)}} [\log p(\mathbf{W}^{(S)} | \boldsymbol{\Gamma}^{(S)}) p(\boldsymbol{\Gamma}^{(S)} | \boldsymbol{\eta}^{(S)}) p(\boldsymbol{\eta}^{(S)})] + \log p(\boldsymbol{\Sigma}), \right. \end{aligned} \quad (2.4)$$

where $\Theta = \{\theta, \psi_S, \psi_m, \mathbf{W}^{(S)}, \mathbf{W}^{(m)}, \boldsymbol{\eta}^{(S)}, \boldsymbol{\eta}^{(m)}, \boldsymbol{\Sigma}\}_{m=1}^M$ and D_{KL} is the Kullback-Leibler divergence.

To optimize Eq. 2.4, we alternate between an expectation step and a maximization step. In the expectation step, we calculate expectations with respect to latent indicators $\boldsymbol{\Gamma}$ and latent factors $\{\mathbf{z}_i^{(m)}, \boldsymbol{\zeta}_i^{(m)}\}_{i,m=1}^{n_m, M}$. In the maximization step, we take gradient steps in model parameters and variational parameters with the help of reparameterization gradients (Kingma and Welling, 2014; Rezende et al., 2014). For more details see § B.

2.4 Negative-Binomial MSSVAE

To accommodate for overdispersed count data as in the RNA-seq data example, we additionally consider a multi-study DGM with a negative-binomial likelihood. Specifically, the observed data is distributed as:

$$\mathbf{x}_{ij}^{(m)} | \widetilde{\mathbf{w}}_j^{(m)}, \widetilde{\mathbf{z}}_i^{(m)}, \phi_j \sim \text{NB}(\text{mean} = \ell_i^{(m)} f_{\theta, j}(\widetilde{\mathbf{w}}_j^{(m)} \odot \widetilde{\mathbf{z}}_i^{(m)}), \text{inv-disp} = \phi_j) \quad (2.5)$$

where $\ell_i^{(m)}$ is the library size (i.e. sum of transcripts in sample i of study m) and ϕ_j is the per-gene inverse dispersion. To ensure the mean is positive, the neural network f_{θ} applies to the final layer an element-wise softplus function: $\text{softplus}(z) = \log(1 + \exp(z))$. We use a parameterization of the negative-binomial distribution with the following probability mass function (for mean μ , inverse-dispersion ϕ):

$$p_{NB}(x; \mu, \phi) = \frac{\Gamma(x + \phi)}{\Gamma(x + 1)\Gamma(\phi)} \left(\frac{\phi}{\phi + \mu} \right)^{\phi} \left(\frac{\mu}{\phi + \mu} \right)^x.$$

We choose this parameterization as it was noted to be computationally stable for genomics data (Lopez et al., 2018). Also following Lopez et al. (2018), we take the prior on ℓ_i to be:

$$\ell_i \sim \text{LogNormal}(\ell_\mu, \ell_\sigma^2),$$

where ℓ_μ, ℓ_σ^2 are set to the empirical mean and variance of the observed library sizes, $\{\sum_{j=1}^G x_{ij}\}_{i=1}^n$. We estimate ℓ_i using variational inference; the variational distribution is:

$$q(\ell_i | \mathbf{x}_i) = \text{LogNormal}(\mu_\ell(\mathbf{x}_i), \sigma_\ell^2(\mathbf{x}_i)),$$

where $\mu_\ell, \sigma_\ell^2 : \mathbb{R}^G \rightarrow \mathbb{R}$ are neural networks.

The negative-binomial MSSVAE is fit using the same objective as in Eq. 2.4, replacing the Gaussian likelihood with the negative binomial, subtracting the Kullback-Leibler divergence $D_{KL}(q(\ell_i^{(m)} | \mathbf{x}_i^{(m)}) || p(\ell_i^{(m)}))$, and omitting the noise variance Σ terms. The inverse-dispersion parameters $\{\phi_j\}_{j=1}^G$ are not assigned a prior but are also estimated in the optimization the MAP objective.

3 Identifiability

Identifiability is important for reliability and interpretability of the latent variables. We first consider a single-study deep generative model, and strengthen existing identifiability results from Moran et al. (2022). Using these results, we then consider the multi-study deep generative model, and prove identifiability of the shared and study-specific masking matrices.

3.1 Single-Study Model

A single-study generative model with additive Gaussian noise is:

$$\mathbf{x}_i = f(\mathbf{z}_i) + \boldsymbol{\varepsilon}_i, \quad \boldsymbol{\varepsilon}_i \stackrel{ind}{\sim} N_G(\mathbf{0}, \Sigma), \quad \Sigma = \text{diag}\{\sigma_j\}_{j=1}^G, \quad i = 1, \dots, N, \quad (3.1)$$

where $\mathbf{z}_i \sim p_{\mathbf{z}} \in \mathcal{P}_z$ and $f \in \mathcal{F}$, with \mathcal{P}_z denoting a class of probability distributions and \mathcal{F} denoting a class of functions.

There are three main identifiability issues in the model Eq. 3.1. First, the noise variance Σ is unknown. Second, the latent factor dimension is generally unknown. Third, we can always re-parameterize the model:

$$\mathbf{x}_i = f(h^{-1}(h(\mathbf{z}_i))) + \boldsymbol{\varepsilon}_i, \quad \text{for any invertible } h : \mathbb{R}^K \rightarrow \mathbb{R}^K, \quad (3.2)$$

when $f \odot h^{-1} \in \mathcal{F}$ and $h_{\#} p_{\mathbf{z}} \in \mathcal{P}_z$, where $h_{\#} p_{\mathbf{z}}$ is the pushforward measure of $p_{\mathbf{z}}$ by h . To restrict possible functions h , we can place restrictions on \mathcal{F} , \mathcal{P}_z , or both.

Our strategy is to restrict \mathcal{F} to a specific set of sparse functions. As discussed in § 2.2, we do so by introducing the parameter \mathbf{w}_j which selects which of the K latent factor dimensions are used to generate x_{ij} :

$$x_{ij} = f_j(\mathbf{w}_j \odot \mathbf{z}_i) + \varepsilon_{ij}, \quad i = 1, \dots, N; \quad j = 1, \dots, G, \quad (3.3)$$

where $\mathbf{w}_j \in \mathbb{R}^K$. If $w_{jk} = 0$, then z_{ik} cannot contribute to x_{ij} . We denote $\mathbf{W} = [\mathbf{w}_1, \dots, \mathbf{w}_G]^T$.

We assume a specific kind of sparsity in \mathbf{W} , corresponding to an anchor feature assumption (Moran et al., 2022). An anchor feature is a dimension of \mathbf{x}_i that depends only on one latent factor dimension. Anchor feature assumptions have also been used for identification in latent topic modeling (Arora et al., 2013), linear factor analysis (Bing et al., 2020, 2023) and nonlinear additive factor analysis (Xu et al., 2023).

Assumption 1 (Anchor features.). *For every non-zero factor dimension $\mathbf{z}_{\cdot k}$, there are at least two features $\mathbf{x}_{\cdot j(k)}$, $\mathbf{x}_{\cdot j'(k)}$ which depend only on that factor. Moreover, the two features have the same mapping from the factors, up to a multiplicative factor $c_{j'(k)}$; that is, for all $i = 1, \dots, N$:*

$$\mathbb{E}[x_{i,j(k)} | \tilde{\mathbf{z}}_i] = f_{j(k)}(z_{ik}), \quad \mathbb{E}[x_{i,j'(k)} | \mathbf{z}_i] = c_{j'(k)} f_{j(k)}(z_{ik}), \quad (3.4)$$

where $f_{j(k)} : \mathbb{R} \rightarrow \mathbb{R}$ are strictly monotone functions. We refer to such features as “anchor features”. Note we have slightly abused notation by using $f_{j(k)}(z_{ik})$ to denote $f([0, \dots, 0, w_{jk}, 0, \dots, 0] \odot [0, \dots, 0, z_{jk}, 0, \dots, 0])_j$; that is, \mathbf{w}_j has only one non-zero entry in dimension k .

Remark 1. *Assumption 1* differs from the anchor assumption in Moran et al. (2022) in two ways. First, here the two anchor features for the same factor dimension have the same mean, up to a multiplicative constant. Moran et al. (2022) has the stricter condition that the two anchor features have the same mean. Secondly, we assume the anchor mappings $f_{j(k)}$ are strictly monotone functions; this is a stronger condition than Moran et al. (2022); we require this assumption to ultimately identify the support of \mathbf{W} , which Moran et al. (2022) do not consider.

Our proof strategy will utilize the “parallel rows” argument of Bing et al. (2023). Specifically, Bing et al. (2023) consider a linear factor model, and prove that rows in the marginal population correlation matrix (excluding diagonal elements) are parallel if and only if corresponding rows of the loadings matrix are parallel (assuming also that the latent factor covariance is rank K).

We extend this “parallel rows” idea to the nonlinear setting. Below, **Assumption 2** assumes that non-anchor features are non-parallel almost everywhere. **Assumption 3** is the analogue

of the covariance of \mathbf{z}_i being rank- K . With these assumptions, the parallel rows of the correlation matrix must correspond to anchor features, allowing anchors to be identified from the marginal correlation matrix.

Assumption 2 (Non-anchor feature differences). *For any two features x_{il}, x_{ip} which are not anchored to a factor, we assume their means are not scalar multiples. That is, for any $c_{lp} \neq 0$, we have*

$$f_l(\mathbf{w}_l \odot \mathbf{z}_i) \neq c_{lp} f_p(\mathbf{w}_p \odot \mathbf{z}_i) \quad \text{almost everywhere.}$$

Assumption 3 (Covariance non-degeneracy). *Define $T_{\mathcal{S}} : L^2(\mathcal{P}_z) \rightarrow \mathbb{R}^{|\mathcal{S}|}$ as the covariance map restricted to a subset of indices $\mathcal{S} \subset \{1, \dots, G\}$:*

$$T_{\mathcal{S}}(m) := (\text{Cov}(m(\mathbf{z}_i), x_{il}))_{l \in \mathcal{S}}.$$

We assume that for any subset \mathcal{S} with $|\mathcal{S}| = G - 2$, and for any linear combination $m \in \text{span}(\mathcal{F})$:

$$T_{\mathcal{S}}(m) = 0 \implies m = 0 \quad \text{almost everywhere.}$$

Next, to identify the entire support of \mathbf{W} , we need some additional assumptions.

Assumption 4 (Conditional latent non-degeneracy). *The conditional distribution $p(z_{ik} | \mathbf{z}_{i, \setminus k})$ is non-atomic almost everywhere, where $\mathbf{z}_{i, \setminus k} = (z_{i1}, \dots, z_{i,k-1}, z_{i,k+1}, \dots, z_{iK})$.*

Assumption 5 (Functional non-degeneracy). *For any $j \in \{1, \dots, G\}$ and $k \in \{1, \dots, K\}$, if $w_{jk} \neq 0$, then the function f_j is not constant with respect to the k th input coordinate on the support of \mathbf{z} .*

Assumptions 4 and 5 ensure that if $w_{jk} \neq 0$, then x_{ij} is not constant with respect to z_{ik} .

Theorem 1. *Suppose Assumptions 1 to 5 hold. Then*

1. *The anchor features and the latent dimensionality K are identifiable from the marginal population correlation matrix.*
2. *For any two solutions $(f, \mathbf{W}, \Sigma, p_z)$, $(\hat{f}, \hat{\mathbf{W}}, \hat{\Sigma}, \hat{p}_z)$ with*

$$p(\mathbf{x}_i | f, \mathbf{W}, \Sigma) = p(\mathbf{x}_i | \hat{f}, \hat{\mathbf{W}}, \hat{\Sigma}),$$

the factors are equal in distribution up to element-wise transformations and permutations:

$$(z_{i1}, \dots, z_{iK}) \stackrel{d}{=} (h_1(\hat{z}_{i,\pi(1)}), \dots, h_K(\hat{z}_{i,\pi(K)})),$$

where $h_k : \mathbb{R} \rightarrow \mathbb{R}$ are invertible functions and $\pi : \{1, \dots, K\} \rightarrow \{1, \dots, K\}$ is a permutation.

3. The support of \mathbf{W} is identifiable, up to permutation of columns.

4. The error variances Σ are identifiable.

The proof is in § A. We provide a proof sketch here. (1) We prove that parallel rows of the marginal correlation matrix (excluding diagonal entries) correspond to anchor features. This allows identification of the anchor features, which correspond to rows of \mathbf{W} which have one non-zero element. (2) Because the anchor features are identified, and they are parallel, we can identify the noise variances corresponding to the anchor features. (3) Then, we can prove the factors are equal in distribution up to an element-wise transform and permutation. (4) We prove by contradiction that under the non-degeneracy Assumptions 4 and 5, the support of \mathbf{W} is identifiable. (5) Finally, we prove the non-anchor noise variances are identified.

Remark 2. Our identification strategy for the anchor features follows [Bing et al. \(2023\)](#), which is a constructive proof. In practice, we do not select anchor features using the marginal correlation matrix. Instead, we take a Bayesian approach and place a sparsity-inducing prior on \mathbf{W} to penalize non-sparse solutions.

Remark 3. Our identifiability proof does not require assumptions on p_z beyond non-degeneracy of the marginal covariance (Assumption 3) and non-degeneracy of the conditional distributions (Assumption 4). For estimation, we adopt standard Gaussian priors for the latent variables. In practice, we have found standard Gaussian priors to perform as well as Gaussian priors with a learned covariance. Consequently, for computational efficiency, we use standard Gaussian priors. Note that the variational distribution $q_\phi(\mathbf{z}_i|\mathbf{x}_i)$ can have dependencies between entries of \mathbf{z}_i , after marginalizing over \mathbf{x}_i .

Remark 4. Our identifiability results consider deep generative models with additive Gaussian noise. For non-additive noise such as the negative binomial model, our results only hold assuming we have identified the signal distribution $f_{\#}p_z$ from the noise.

3.2 Multi-Study Model

We return to the multi-study sparse deep generative model:

$$x_{ij}^{(m)} = f_j(\tilde{\mathbf{w}}_j^{(m)} \odot \tilde{\mathbf{z}}_i^{(m)}) + \varepsilon_{ij}^{(m)}, \quad \varepsilon_i^{(m)} \stackrel{ind}{\sim} N_G(\mathbf{0}, \Sigma), \quad (3.5)$$

where again $\Sigma = \text{diag}(\sigma_1, \dots, \sigma_G^2)$. Recall that $\tilde{\mathbf{W}}^{(m)}$ concatenates the shared matrix $\mathbf{W}^{(S)}$ with the study-specific matrix $\mathbf{W}^{(m)}$. Similarly, $\tilde{\mathbf{z}}_i^{(m)}$ concatenates the shared factors $\mathbf{z}_i^{(m)} \sim p_z \in \mathcal{P}$ and the study-specific factors $\xi_i^{(m)} \sim p_{\xi^{(m)}} \in \mathcal{P}$. That is, the shared factors are drawn from the same p_z , while the study-specific factors are drawn from possibly different distributions $p_{\xi^{(m)}}$.

The multi-study model introduces an identifiability concern beyond those in the single-study model. The central issue is that the model in Eq. 3.5 is observationally equivalent to a misspecified model that has no shared components ($\widehat{\mathbf{W}}^{(S)} = \mathbf{0}$); instead, this shared signal is concatenated with each of the study-specific matrices. This identifiability issue is referred to as “information switching” by Chandra et al. (2025).

For the multi-study deep generative model, we prove that we can identify the shared signal from the study-specific signal.

Theorem 2. *Suppose Assumptions 1 to 5 hold for each study, considered separately. Then, the supports of the shared matrix $\mathbf{W}^{(S)}$ and study-specific matrices $\mathbf{W}^{(m)}$ are identifiable.*

The proof is in § A. First, we consider each study separately and utilize Theorem 1 to obtain identifiability of the supports of each $\widehat{\mathbf{W}}^{(m)}$, up to permutation of columns. (Note that this does not yet distinguish the shared from the study-specific signal due to column permutations.) Second, we construct the shared matrix $\mathbf{W}^{(S)}$ from the columns that are equal across all studies. The remaining columns form the study-specific matrices $\{\widehat{\mathbf{W}}^{(m)}\}_{m=1}^M$. This proof is constructive and similar in spirit to Sturma et al. (2023); Mauri et al. (2025).

Remark 5. *In the linear multi-study setting, Chandra et al. (2025) prove that information switching occurs if and only if either (i) the intersection of the column space of the study-specific matrices $\{\mathbf{W}^{(m)}\}_{m=1}^M$ is non-null, or (ii) $\text{rank}(\mathbf{W}^{(m)}) < K_m$ for all m . This is not contradicted in our result. For (i), because of the construction of $\mathbf{W}^{(S)}$, the remaining $\mathbf{W}^{(m)}$ have column spaces whose intersection is null. For (ii), $\mathbf{W}^{(m)}$ have full rank because of the anchor assumption.*

Remark 6. *While the identifiability proof is constructive, in practice we take a Bayesian approach and induce sparsity in $\mathbf{W}^{(S)}, \{\mathbf{W}^{(m)}\}_{m=1}^M$. This encourages the shared signal to be estimated in $\mathbf{W}^{(S)}$ instead of $\{\mathbf{W}^{(m)}\}_{m=1}^M$. This is because placing the shared signal in $\{\mathbf{W}^{(m)}\}_{m=1}^M$ requires $M - 1$ additional non-sparse columns over the solution with shared signal in $\mathbf{W}^{(S)}$.*

4 Simulation studies

We consider two synthetic data experiments: nonlinear factor analysis with Gaussian observations (§ 4.1) and synthetic bulk RNA-sequencing data with gene correlation (§ 4.2).

4.1 Gaussian nonlinear factor analysis

In this simulation study, the observed data is Gaussian, drawn from a nonlinear latent factor model. We have $M = 3$ studies, $N_m = 1000$ samples per study, $G = 100$ features,

$K_S = 8$ shared latent dimensions and $K_m = 2$ study-specific latent dimensions for each $m \in \{1, \dots, M\}$.

In this data, every third feature has a nonlinear relationship with the latent factors. Specifically, for $m = 1, \dots, M$, $i = 1, \dots, N_m$ and $j = 1, \dots, G$:

$$x_{ij}^{(m)} = \begin{cases} \sum_{k=1}^{K_S} W_{jk}^{(S)} z_{ik}^{(m)} + \sum_{k=1}^{K_m} W_{jk}^{(m)} \xi_{ik}^{(m)} + \varepsilon_{ij}^{(m)} & \text{if } j \not\equiv 0 \pmod{3} \\ \sum_{k=1}^{K_S} W_{jk}^{(S)} (z_{ik}^{(m)})^2 + \sum_{k=1}^{K_m} W_{jk}^{(m)} (\xi_{ik}^{(m)})^2 + \varepsilon_{ij}^{(m)} & \text{if } j \equiv 0 \pmod{3} \end{cases}$$

where $\varepsilon_{ij}^{(m)} \sim \mathcal{N}(0, 0.2)$. The latent factors are generated as $\mathbf{z}_i^{(m)} \sim \mathcal{N}_{K_S}(\mathbf{0}, 0.5^2 \cdot \mathbf{I})$ and $\boldsymbol{\xi}_i^{(m)} \sim \mathcal{N}_{K_m}(\mathbf{0}, 0.5^2 \cdot \mathbf{I})$. The matrices $\mathbf{W}^{(S)}, \{\mathbf{W}^{(m)}\}_{m=1}^M$ have a sparse structure displayed in [Figure 2b](#). The non-zero entries are $w_{jk}^{(S)} \stackrel{iid}{\sim} N(8, 0.01)$ and $w_{jk}^{(m)} \stackrel{iid}{\sim} N(10, 0.01)$.

To measure performance of the MSSVAE, we report the consensus score ([Hochreiter et al., 2010](#)), relevance and recovery ([Prelić et al., 2006](#)), and the disentanglement score ([Eastwood and Williams, 2018](#)). The consensus score measures how similar the estimated $\widehat{\mathbf{W}}$ are to the support of the true \mathbf{W} , penalizing overestimation of the support. Relevance measures how similar on average the estimated column supports are to the true support (cf. precision). Recovery instead measures how similar on average the true column supports are to the estimated supports (cf. recall). The disentanglement score is an average measure of how relevant each estimated factor is for a true factor, penalizing estimated factors that are informative of multiple true factors (i.e. “entangling” multiple true factors). For precise definitions, see [§ C](#).

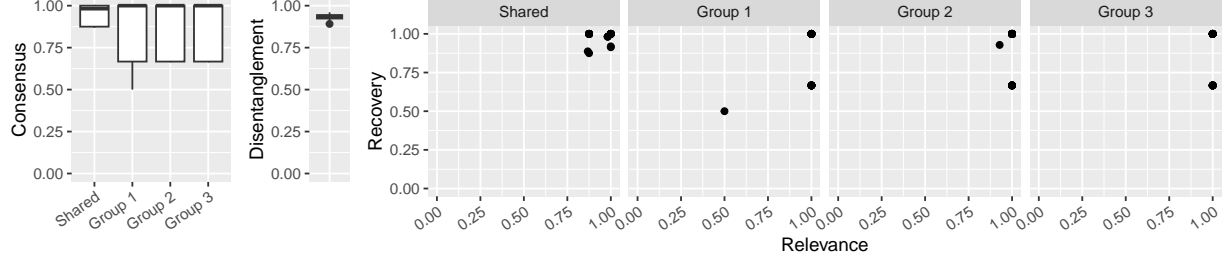
The MSSVAE has high consensus, relevance and recovery, and disentanglement scores, measured on 30 different simulated datasets ([Figure 2a](#)). We visualize the output of one of the 30 experiments in [Figure 2c](#); here, MSSVAE successfully estimates the sparse structure and nonlinear mapping, even when using an overestimate of the true latent dimensions. In the appendix, we display the worst performing of the 30 experiments in terms of average consensus score ([Figure 6](#)).

4.2 Synthetic Bulk RNA-Sequencing Data

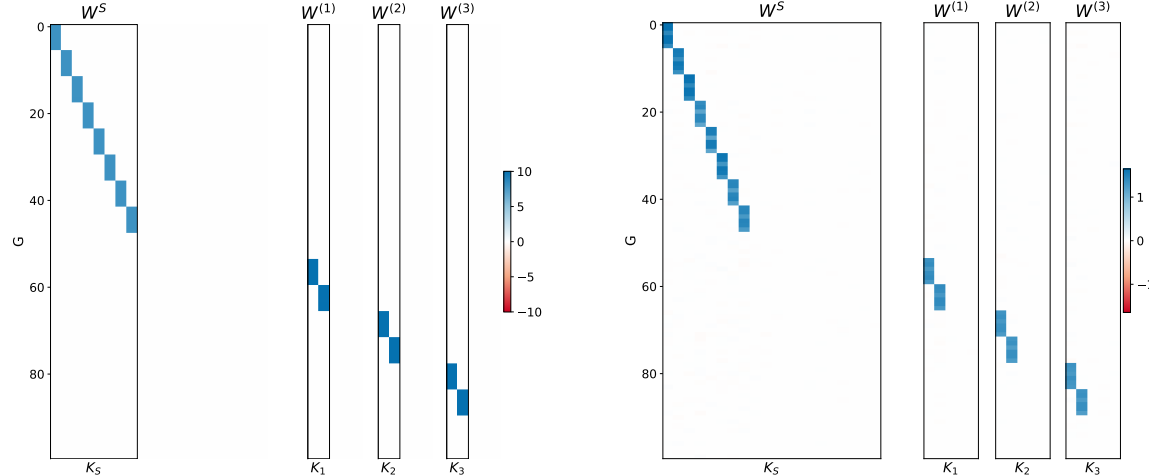
In this simulation study, we consider synthetic bulk RNA-sequencing data. This synthetic data is generated similarly to [Zappia et al. \(2017\)](#), omitting dropout variation, which is specific to single-cell data.

We have $N = 3200$ samples, $G = 5000$ features and $M = 3$ groups, with the proportion of samples in each group set to (30%, 30%, 40%).

First, the base expression for gene j in sample i of group m , is generated from latent factors

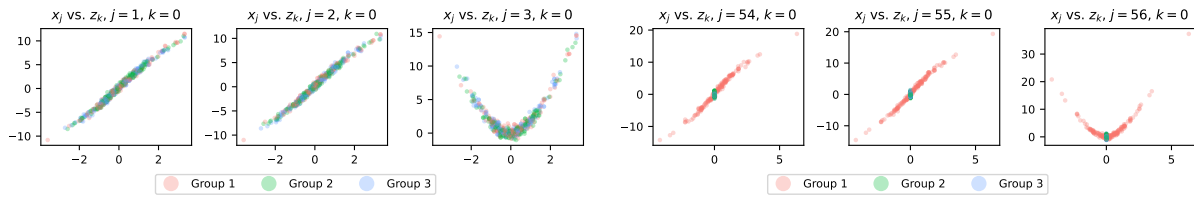


(a) MSSVAE results over 30 different synthetic datasets. Consensus and relevance/recovery are separated into shared and group structure; disentanglement is over all factors. All metrics are in $[0,1]$; higher is better.



(b) True $\mathbf{W}^S, \mathbf{W}^{(m)}$.

(c) Estimated $\widehat{\mathbf{W}}^{(S)}, \widehat{\mathbf{W}}^{(m)}$.



(d) Data vs. shared factors.

(e) Data vs. study-1 factors.

Figure 2: Gaussian nonlinear factor analysis. (a) Results over 30 replications. (b-e) Result of one replication as an example. MSSVAE successfully estimates \mathbf{W} , including factor dimension (after removing columns of all zeros).

as:

$$\mu_{ij}^{(m)} = \begin{cases} b_j + \sum_{k=1}^{K_S} W_{jk}^{(S)} z_{ik}^{(m)} + \sum_{k=1}^{K_m} W_{jk}^{(m)} \xi_{ik}^{(m)} & \text{if } j \not\equiv 0 \pmod{3} \\ b_j + \sum_{k=1}^{K_S} W_{jk}^{(S)} \sin(3\pi/4 \cdot z_{ik}^{(m)}) + \sum_{k=1}^{K_m} W_{jk}^{(m)} \sin(3\pi/4 \cdot \xi_{ik}^{(m)}) & \text{if } j \equiv 0 \pmod{3} \end{cases}$$

where $b_j \sim N(0, 0.5^2)$ is a gene-specific intercept. The matrices $\mathbf{W}^{(S)}, \{\mathbf{W}^{(m)}\}_{m=1}^M$ have a mostly block structure with 5% non-block, non-zero elements (see [Figure 3b](#) for an example). The non-zero elements are drawn as $w_{jk}^{(S)} \stackrel{iid}{\sim} N(10, 0.01)$ and $w_{jk}^{(m)} \stackrel{iid}{\sim} N(12, 0.01)$.

To ensure base expression is positive, we then apply a softplus function. Then, we normalize so the gene expression levels for each sample sum to one:

$$\mu_{ij}^{(m)'} = \frac{\log(1 + \exp(\mu_{ij}^{(m)}))}{\sum_{j=1}^G \log(1 + \exp(\mu_{ij}^{(m)}))}.$$

This normalization induces correlation among all genes, making it more difficult to learn the true \mathbf{W} matrices.

Next, the library size for each sample i is generated as $\ell_i \sim \text{LogNormal}(12, 0.5^2)$. The sample mean is then calculated as $\tilde{\mu}_{ij}^{(m)} = \ell_i \mu_{ij}^{(m)'}$.

To model the mean-variance trend in RNA-sequencing data ([McCarthy et al., 2012](#)), we follow [Zappia et al. \(2017\)](#) and simulate the biological coefficient of variation for each gene from a scaled inverse chi-squared distribution:

$$\text{BCV}_{ij}^{(m)} = \left(\phi + 1/\sqrt{\tilde{\mu}_{ij}^{(m)}} \right) \sqrt{\nu/q_{ij}^{(m)}}, \quad q_{ij}^{(m)} \sim \chi_\nu^2,$$

with $\phi = 0.1$ and $\nu = 60$.

Finally, the observed data is generated as:

$$X_{ij}^{(m)} \sim \text{NB}(\text{mean} = \tilde{\mu}_{ij}^{(m)}, \text{inv-disp} = 1/(\text{BCV}_{ij}^{(m)})^2).$$

To this data, we fit the Negative-Binomial MSSVAE ([Eq. 2.5](#)). We initialize the latent dimensions to be $\widetilde{K}^{(S)} = 50$ and $\widetilde{K}^{(m)} = 10$ for all $m = 1, \dots, M$.

For 30 different generated datasets, we fit the NB-MSSVAE and calculate the consensus, relevance, recovery and disentanglement scores. Due to the correlation induced among genes by the normalization, there are some columns of $\mathbf{W}^{(S)}$ that are dense; consequently, we remove columns with greater than 25% non-zero elements when calculating the consensus, relevance and recovery scores.

The NB-MSSVAE has good consensus, disentanglement, relevance and recovery scores over 30 different synthetic datasets, albeit lower than the Gaussian example ([Figure 3a](#)).

This performance gap is due to the more difficult setting with overdispersed count data, per-sample library size effects, and correlation between genes induced by the per-sample normalization. We visualize the output of one of the 30 experiments in [Figure 3c](#); here, the NB-MSSVAE estimates the sparse structure well, although the shared latent dimension is overestimated.

5 Platelet Data

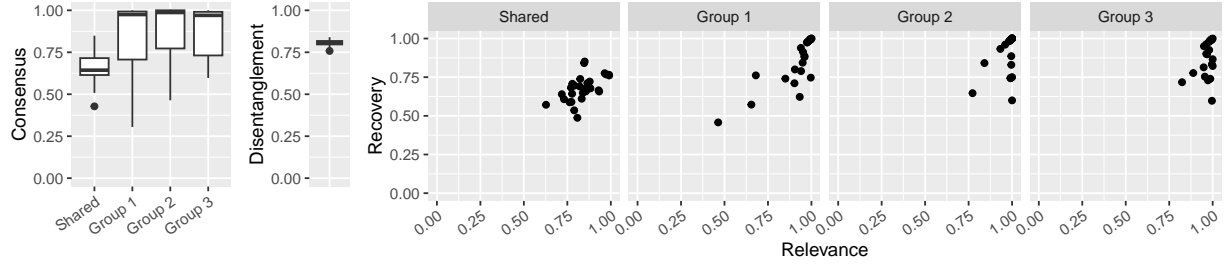
In this section, we analyze platelet transcriptomes from a multi-disease cohort of $N = 1,463$ ancestrally diverse patients. This dataset, curated from publications across collaborator labs ([Gao et al., 2022](#); [Sol et al., 2020](#); [Best et al., 2015, 2017, 2018](#); [Rowley et al., 2019](#); [Voora et al., 2014](#)), spans $M = 6$ disease categories: cardiovascular disease, multiple sclerosis (immune-mediated), non-small-cell lung cancer, glioblastoma, other cancers (Table 1), contrasted with healthy donors. This disease spectrum enables systematic investigation of shared platelet molecular pathways versus disease-specific transcriptomic signatures across conditions ranging from cardiovascular dysfunction to malignancy-associated thrombosis. We consider the top $G = 5000$ most variable genes based on Pearson residuals of a negative binomial offset model ([Lause et al., 2021](#)), implemented using `scipy` ([Wolf et al., 2018](#)). This filtering step enriches for genes with meaningful biological variation across disease states and individuals, prioritizing genes likely to capture disease-related and platelet-specific transcriptomic signatures while reducing noise from constitutively expressed genes.

Group	Count
Healthy	437
Cardiovascular Disease	61
Multiple Sclerosis	92
Non Small Cell Lung Cancer	299
Glioblastoma	286
Other Cancer	288
Total	1463

Table 1: Platelet RNA-seq cohort composition by disease group (N=1,463).

To this data, we fit the NB-MSSVAE and obtain $\widehat{\mathbf{W}}^{(S)}, \{\widehat{\mathbf{W}}^{(m)}\}_{m=1}^M$. For each factor k , we select genes with W_{gk} values above a threshold: $\mathcal{C}_k = \{g \in \{1, \dots, G\} : |W_{g,k}| > 0.5\}$.

To evaluate the biological significance of these gene sets $\{\mathcal{C}_k\}_{k=1}^K$, we conduct gene overrepresentation tests ([Xu et al., 2024](#)). That is, we test whether known gene pathways occur in the selected set \mathcal{C}_k more often than expected by chance using Fisher’s exact test, with p -values adjusted for multiple testing using the Benjamini-Yekutieli procedure ([Benjamini](#)



(a) MSSVAE results over 30 different synthetic datasets. Consensus and relevance/recovery are separated into shared and group structure; disentanglement is over all factors. All metrics are in $[0,1]$; higher is better.

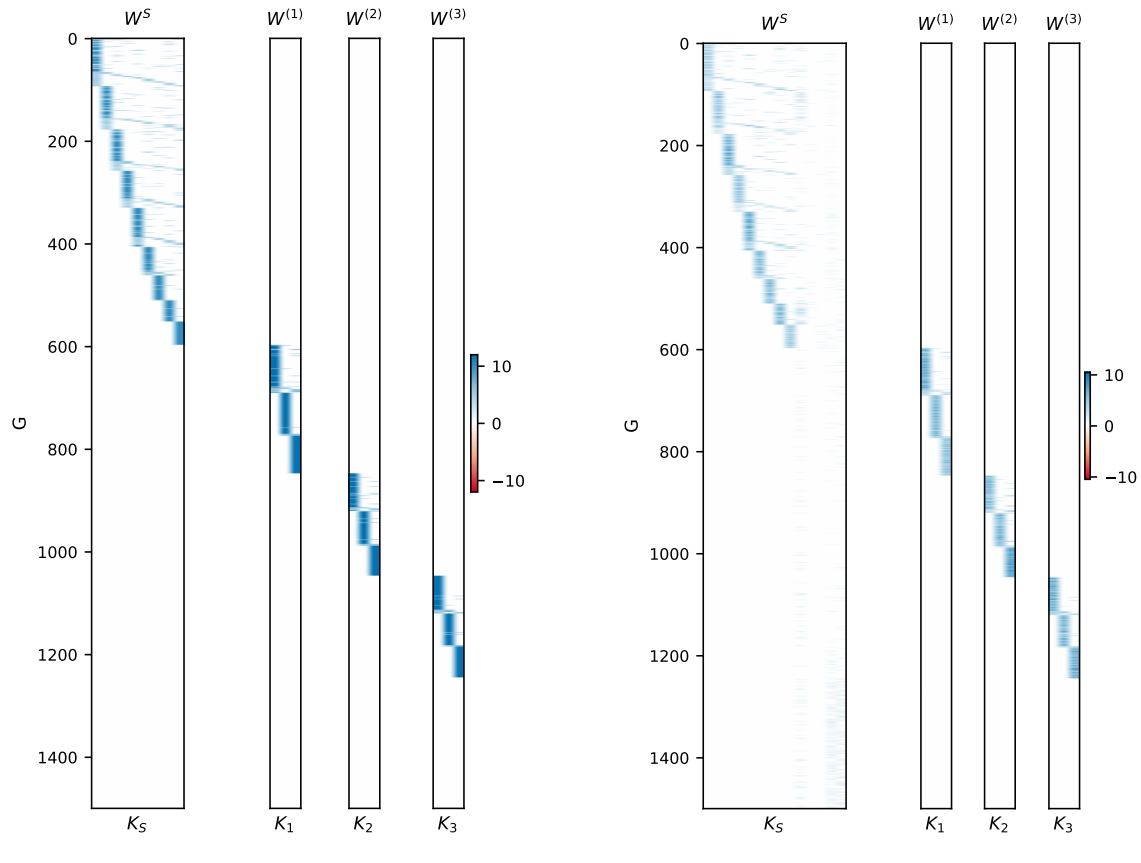


Figure 3: Synthetic gene expression data. (a) Results over 30 replications. (b-e) Result of one replication as an example.

and Yekutieli, 2001). For the known gene groups, we use Gene Ontology Biological Processes. The tests were implemented using `clusterProfiler` (Xu et al., 2024).

Of the gene sets corresponding to the shared factor dimensions, 96% were significantly enriched for at least one Gene Ontology Biological Process (FDR < 0.05). The enriched processes include fundamental platelet functions: hemostasis, thrombosis, inflammatory response, and immune response, along with essential cellular processes including cell metabolism, protein synthesis, and cell-cycle regulation. For each cluster, Figure 4 shows the top 3 biological processes for each latent by effect size (i.e. fold enrichment), after filtering for processes appearing in more than 10% of clusters. These shared factors represent conserved molecular pathways active across all disease states, likely reflecting core platelet biology and ubiquitous systemic stress responses.

Of the disease-specific clusters, 56% were enriched for at least one Gene Ontology Biological Process (FDR < 0.05). The lower percentage is due to many clusters containing fewer than 5 genes (10/60). The biological processes are broadly consistent with the disease-state:

- Healthy clusters are enriched for housekeeping-type processes e.g. RNA processing.
- Cardiovascular clusters are enriched for oxidative stress (i.e. response to hydrogen peroxide).
- Multiple Sclerosis (immune-mediated) clusters are enriched for immune related processes such as Type I interferon signaling, response to viruses, and innate immune response.
- Cancer clusters (glioblastoma, NSCLC, other cancer) are enriched for stress signaling (e.g. intrinsic apoptotic signaling) and inflammation (NF-kappaB signaling).

For each cluster, Figure 5 shows the top 5 biological processes by fold enrichment, after filtering for processes appearing in more than 10% of clusters. This separation of shared and disease-specific biological processes demonstrates the utility of the MSSVAE for understanding disease-specific platelet dysfunction mechanisms while identifying universal platelet biomarkers.

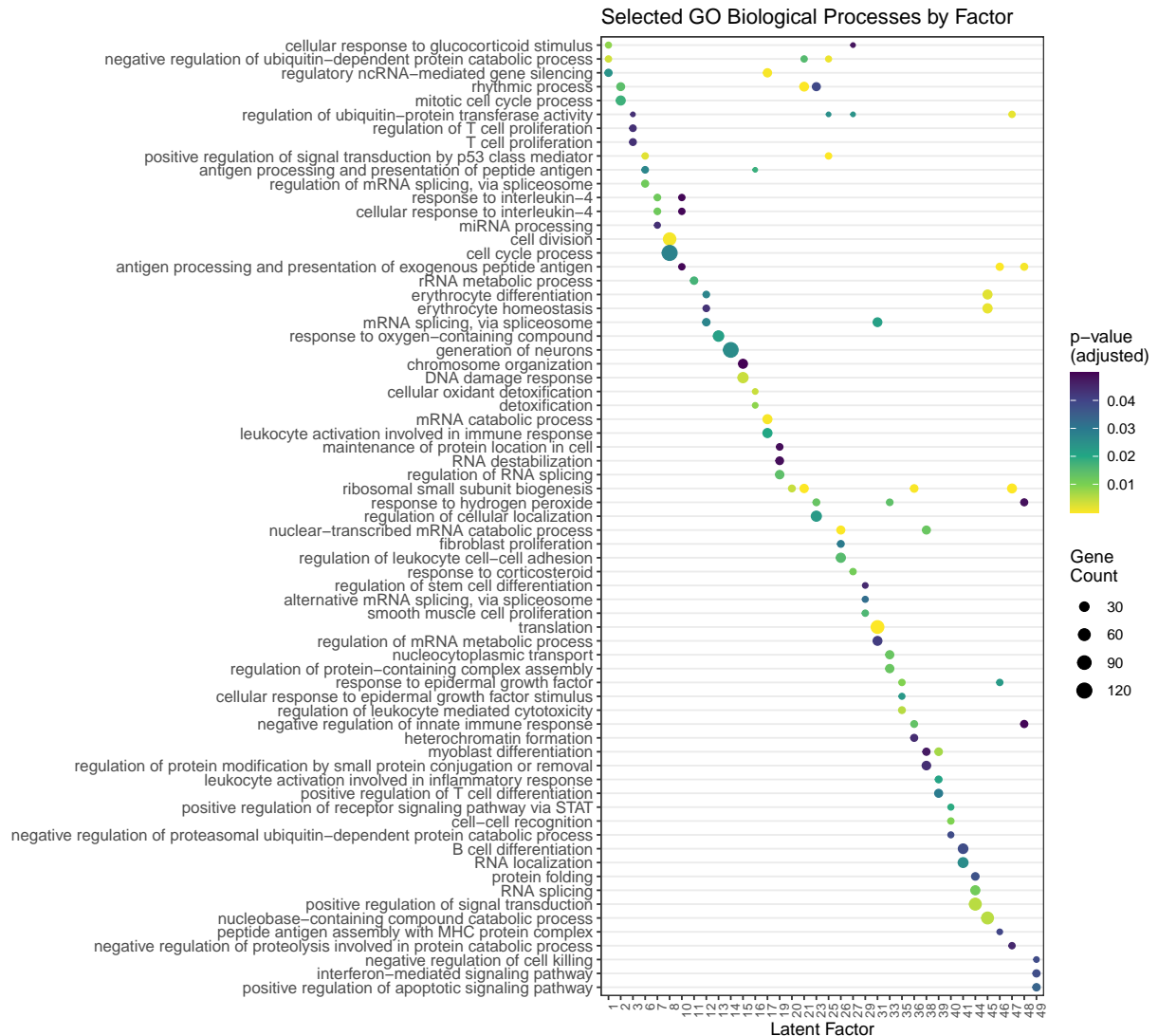


Figure 4: Summary of gene over-representation results for shared latent dimensions. For each latent dimension, we plot the top 3 biological processes by fold enrichment, after filtering for biological processes occurring in more than 10% of latent dimensions.

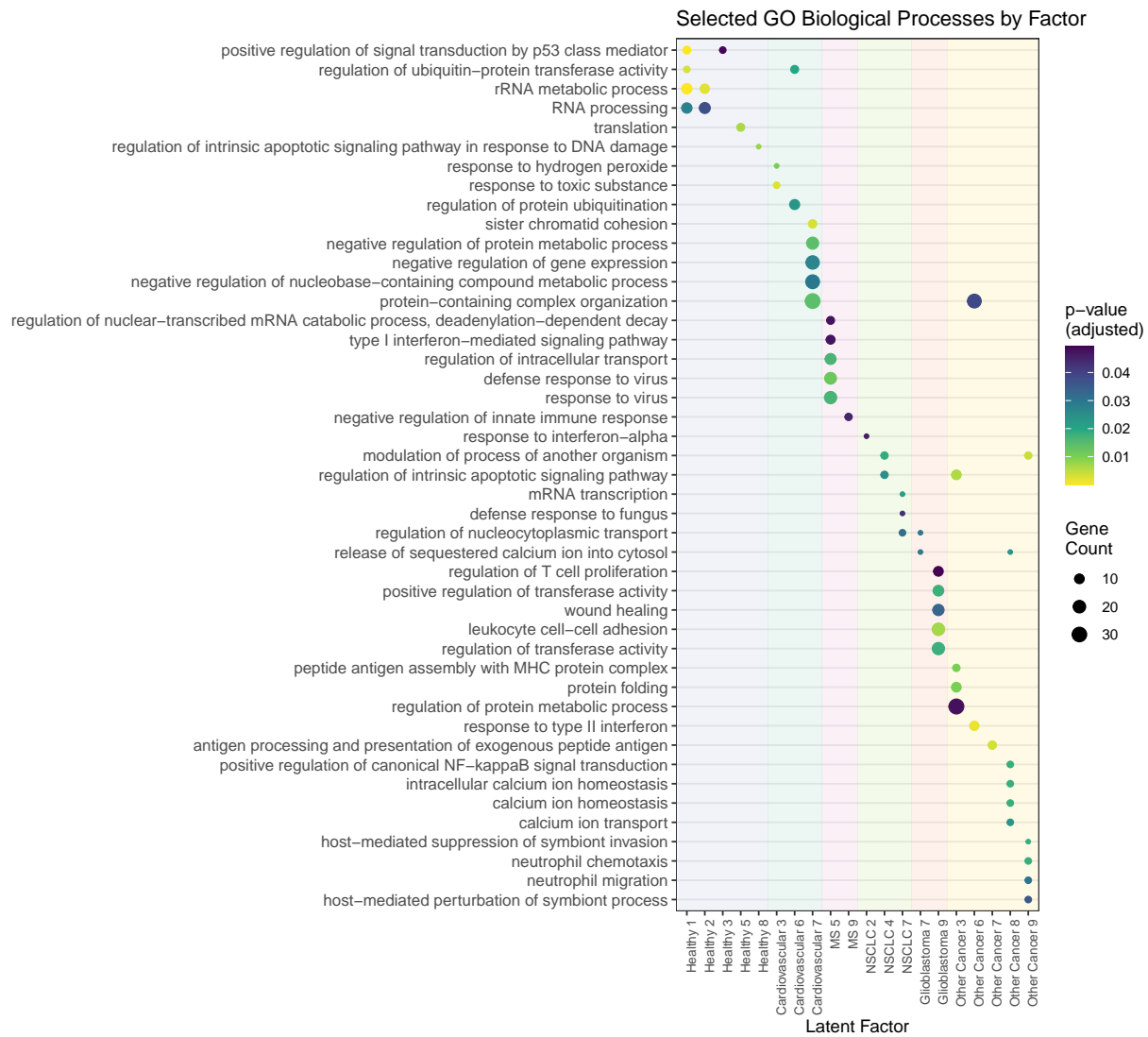


Figure 5: Summary of gene over-representation results for disease-state-specific latent dimensions. Displayed are the top 5 biological processes for each latent dimension by fold enrichment, after filtering for biological processes occurring in more than 10% of latent dimensions.

6 Conclusion

We developed the multi-study sparse deep generative model. The model has spike-and-slab lasso priors that induce sparsity in the mapping from the latent factors to the observed features. The model has sparse mappings corresponding to both a shared latent space among studies, and study-specific latent spaces, allowing for the latent spaces to be interpreted based on the observed features. We prove that the multi-study sparse DGM is identifiable, using an anchor feature assumption. To fit the multi-study sparse DGM, we develop the MSSVAE, both for Gaussian and Negative-Binomial valued data. On synthetic data, we show the MSSVAE can recover the true latent factors, as well as the feature-factor associations. Further, MSSVAE successfully decomposes platelet transcriptomes into shared universal pathways active across disease states and disease-specific transcriptomic dysregulation. This framework enables identification of biomarkers and therapeutic targets specific to individual diseases while recognizing conserved platelet biology fundamental to hemostasis and thrombosis.

References

Arora, S., Ge, R., Halpern, Y., Mimno, D., Moitra, A., Sontag, D., Wu, Y., and Zhu, M. (2013). A practical algorithm for topic modeling with provable guarantees. In *International Conference on Machine Learning*.

Benjamini, Y. and Yekutieli, D. (2001). The control of the false discovery rate in multiple testing under dependency. *The Annals of Statistics*, 29(4):1165–1188.

Best, M. G., Sol, N., In 't Veld, S. G., Vancura, A., Muller, M., Niemeijer, A.-L. N., Fejes, A. V., Tjon Kon Fat, L.-A., Huis In 't Veld, A. E., Leurs, C., Le Large, T. Y., Meijer, L. L., Kooi, I. E., Rustenburg, F., Schellen, P., Verschueren, H., Post, E., Wedekind, L. E., Bracht, J., Esenkbrink, M., Wils, L., Favaro, F., Schoonhoven, J. D., Tannous, J., Meijers-Heijboer, H., Kazemier, G., Giovannetti, E., Reijneveld, J. C., Idema, S., Killestein, J., Heger, M., de Jager, S. C., Urbanus, R. T., Hoefer, I. E., Pasterkamp, G., Mannhalter, C., Gomez-Arroyo, J., Bogaard, H.-J., Noske, D. P., Vandertop, W. P., van den Broek, D., Ylstra, B., Nilsson, R. J. A., Wesseling, P., Karachaliou, N., Rosell, R., Lee-Lewandrowski, E., Lewandrowski, K. B., Tannous, B. A., de Langen, A. J., Smit, E. F., van den Heuvel, M. M., and Wurdinger, T. (2017). Swarm Intelligence-Enhanced Detection of Non-Small-Cell Lung Cancer Using Tumor-Educated Platelets. *Cancer Cell*, 32(2):238–252.e9. Publisher: Elsevier.

Best, M. G., Sol, N., Kooi, I., Tannous, J., Westerman, B. A., Rustenburg, F., Schellen, P., Verschueren, H., Post, E., Koster, J., Ylstra, B., Ameziane, N., Dorsman, J., Smit, E. F., Verheul, H. M., Noske, D. P., Reijneveld, J. C., Nilsson, R. J. A., Tannous, B. A.,

Wesseling, P., and Wurdinger, T. (2015). RNA-Seq of Tumor-Educated Platelets Enables Blood-Based Pan-Cancer, Multiclass, and Molecular Pathway Cancer Diagnostics. *Cancer Cell*, 28(5):666–676. Publisher: Elsevier.

Best, M. G., Wesseling, P., and Wurdinger, T. (2018). Tumor-educated platelets as a noninvasive biomarker source for cancer detection and progression monitoring. *Cancer Research*, 78(13):3407–3412.

Bing, X., Bunea, F., Ning, Y., and Wegkamp, M. (2020). Adaptive estimation in structured factor models with applications to overlapping clustering. *Annals of Statistics*, 48(4):2055–2081.

Bing, X., Bunea, F., and Wegkamp, M. (2023). Detecting approximate replicate components of a high-dimensional random vector with latent structure. *Bernoulli*, 29(2):1368–1391.

Carroll, R. J. and Hall, P. (1988). Optimal rates of convergence for deconvolving a density. *Journal of the American Statistical Association*, 83(404):1184–1186.

Chandra, N. K., Dunson, D. B., and Xu, J. (2025). Inferring covariance structure from multiple data sources via subspace factor analysis. *Journal of the American Statistical Association*, 120(550):1239–1253.

Davison, J., Severson, K., and Ghosh, S. (2019). Cross-population variational autoencoders. In *4th Workshop on Bayesian Deep Learning (NeurIPS)*.

De Vito, R., Bellio, R., Trippa, L., and Parmigiani, G. (2019). Multi-study factor analysis. *Biometrics*, 75(1):337–346.

De Vito, R., Bellio, R., Trippa, L., and Parmigiani, G. (2021). Bayesian multistudy factor analysis for high-throughput biological data. *The Annals of Applied Statistics*, 15(4):1723–1741.

Eastwood, C. and Williams, C. K. (2018). A framework for the quantitative evaluation of disentangled representations. In *International Conference on Learning Representations*.

Gao, Y., Liu, C.-J., Li, H.-Y., Xiong, X.-M., Li, G.-L., In 't Veld, S. G. J. G., Cai, G.-Y., Xie, G.-Y., Zeng, S.-Q., Wu, Y., Chi, J.-H., Liu, J.-H., Zhang, Q., Jiao, X.-F., Shi, L.-L., Lu, W.-R., Lv, W.-G., Yang, X.-S., Piek, J. M. J., de Kroon, C. D., Lok, C. A. R., Supernat, A., Łapińska Szumczyk, S., Łojkowska, A., Żaczek, A. J., Jassem, J., Tannous, B. A., Sol, N., Post, E., Best, M. G., Kong, B.-H., Xie, X., Ma, D., Wurdinger, T., Guo, A.-Y., and Gao, Q.-L. (2022). Platelet RNA enables accurate detection of ovarian cancer: an intercontinental, biomarker identification study. *Protein & Cell*, 14(8):579–590.

Grabski, I. N., De Vito, R., Trippa, L., and Parmigiani, G. (2023). Bayesian combinatorial multistudy factor analysis. *The Annals of Applied Statistics*, 17(3):2212.

Griffiths, T. L. and Ghahramani, Z. (2005). Infinite latent feature models and the Indian buffet process. In *Neural Information Processing Systems*.

Hansen, B., Avalos-Pacheco, A., Russo, M., and Vito, R. D. (2025). Fast variational inference for bayesian factor analysis in single and multi-study settings. *Journal of Computational and Graphical Statistics*, 34(1):96–108.

Hochreiter, S., Bodenhofer, U., Heusel, M., Mayr, A., Mitterecker, A., Kasim, A., Khamiakova, T., Van Sanden, S., Lin, D., Talloen, W., et al. (2010). Fabia: factor analysis for bicluster acquisition. *Bioinformatics*, 26(12):1520–1527.

Ioffe, S. and Szegedy, C. (2015). Batch normalization: Accelerating deep network training by reducing internal covariate shift. In *International Conference on Machine Learning*.

Jerby-Arnon, L., Tooley, K., Escobar, G., Dandekar, G., Madi, A., Goldschmidt, E., Lambden, C., Rozenblatt-Rosen, O., Anderson, A. C., and Regev, A. (2021). Pan-cancer mapping of single t cell profiles reveals a tcf1:cxcr6-cxcl16 regulatory axis essential for effective anti-tumor immunity. *bioRxiv:2021.10.31.466532*.

Kingma, D. P. and Ba, J. L. (2015). Adam: A method for stochastic optimization. In *International Conference on Learning Representations*.

Kingma, D. P. and Welling, M. (2014). Auto-encoding variational Bayes. In *International Conference on Learning Representations*.

Krishnan, A. and Best, M. (2025). Next-generation sequencing of educated platelets for cancer diagnosis and beyond. In Gresele, P., López, J. A., Angiolillo, D. J., and Page, C. P., editors, *Platelets in Thrombotic and Non-Thrombotic Disorders: Pathophysiology, Pharmacology and Therapeutics*, pages 1055–1074. Springer, Invited Book Chapter.

Lause, J., Berens, P., and Kobak, D. (2021). Analytic pearson residuals for normalization of single-cell RNA-seq UMI data. *Genome biology*, 22(1):258.

Lopez, R., Regier, J., Cole, M. B., Jordan, M. I., and Yosef, N. (2018). Deep generative modeling for single-cell transcriptomics. *Nature Methods*, 15(12):1053–1058.

Mauri, L., Anceschi, N., and Dunson, D. B. (2025). Spectral decomposition-assisted multi-study factor analysis. *arXiv preprint arXiv:2502.14600*.

McCarthy, D. J., Chen, Y., and Smyth, G. K. (2012). Differential expression analysis of multifactor RNA-Seq experiments with respect to biological variation. *Nucleic acids research*, 40(10):4288–4297.

Moran, G., Sridhar, D., Wang, Y., and Blei, D. (2022). Identifiable deep generative models via sparse decoding. *Transactions on Machine Learning Research*.

Munkres, J. (1957). Algorithms for the assignment and transportation problems. *Journal of the Society for Industrial and Applied Mathematics*, 5(1):32–38.

Prelić, A., Bleuler, S., Zimmermann, P., Wille, A., Bühlmann, P., Gruissem, W., Hennig, L., Thiele, L., and Zitzler, E. (2006). A systematic comparison and evaluation of biclustering methods for gene expression data. *Bioinformatics*, 22(9):1122–1129.

Rezende, D. J., Mohamed, S., and Wierstra, D. (2014). Stochastic backpropagation and approximate inference in deep generative models. In *International Conference on Machine Learning*.

Ročková, V. and George, E. I. (2018). The spike-and-slab lasso. *Journal of the American Statistical Association*, 113(521):431–444.

Rowley, J. W., Weyrich, A. S., and Bray, P. F. (2019). 7 - the platelet transcriptome in health and disease. In Michelson, A. D., editor, *Platelets*, pages 139–153. Academic Press, fourth edition.

Sol, N., in 't Veld, S. G., Vancura, A., Tjerkstra, M., Leurs, C., Rustenburg, F., Schellen, P., Verschueren, H., Post, E., Zwaan, K., Ramaker, J., Wedekind, L. E., Tannous, J., Ylstra, B., Killestein, J., Mateen, F., Idema, S., de Witt Hamer, P. C., Navis, A. C., Leenders, W. P., Hoeben, A., Moraal, B., Noske, D. P., Vandertop, W. P., Nilsson, R. J. A., Tannous, B. A., Wesseling, P., Reijneveld, J. C., Best, M. G., and Wurdinger, T. (2020). Tumor-educated platelet RNA for the detection and (pseudo)progression monitoring of glioblastoma. *Cell Reports Medicine*, 1(7):100101.

Sturma, N., Squires, C., Drton, M., and Uhler, C. (2023). Unpaired multi-domain causal representation learning. *Neural Information Processing Systems*.

Thomas, S., Kelliher, S., and Krishnan, A. (2024). Heterogeneity of platelets and their responses. *Research and Practice in Thrombosis and Haemostasis*, 8(2). Publisher: Elsevier.

Voora, D., Ginsburg, G. S., and Åkerblom, A. (2014). Platelet RNA as a novel biomarker for the response to antiplatelet therapy. *Future Cardiology*, 10(1):9–12. PMID: 24344654.

Weinberger, E., Lopez, R., Huetter, J.-C., and Regev, A. (2022). Disentangling shared and group-specific variations in single-cell transcriptomics data with multiGroupVI. In *Proceedings of the 17th Machine Learning in Computational Biology Meeting*.

Weyrich, A. S. (2014). Platelets: more than a sack of glue. *Hematology*, 2014(1):400–403.

Wolf, F. A., Angerer, P., and Theis, F. J. (2018). Scanpy: large-scale single-cell gene expression data analysis. *Genome biology*, 19(1):15.

Xu, M., Winter, S., Herring, A. H., and Dunson, D. B. (2023). Identifiable and interpretable nonparametric factor analysis. *arXiv preprint arXiv:2311.08254*.

Xu, S., Hu, E., Cai, Y., Xie, Z., Luo, X., Zhan, L., Tang, W., Wang, Q., Liu, B., Wang, R., Xie, W., Wu, T., Xie, L., and Yu, G. (2024). Using clusterProfiler to characterize multiomics data. *Nature Protocols*, 19(11):3292–3320.

Zappia, L., Phipson, B., and Oshlack, A. (2017). Splatter: simulation of single-cell RNA sequencing data. *Genome biology*, 18(1):174.

A Proofs

Lemma 1. *Under Assumptions 1 to 3, the anchor features are identifiable from the marginal correlation matrix of the data, $R := \text{Cor}(\mathbf{z}_i)$. Specifically, the off-diagonal rows $R_{l,\setminus\{l,p\}}$ and $R_{p,\setminus\{l,p\}}$ are parallel if and only if l and p are anchor features for the same factor.*

Proof. We first prove that if we have anchor features, then their corresponding rows of the correlation matrix are parallel. For anchor features $j(k), j'(k)$, we have $f_{j(k)}(z_{ik}) = c_{j'(k)}f_{j'(k)}(z_{ik})$ for some $c_{j'(k)} \neq 0$. For any other feature l , the noise ε_{il} is independent of $\mathbf{z}_i, \varepsilon_{i,j(k)}, \varepsilon_{i,j'(k)}$. Then for all $l \neq j(k), j'(k)$:

$$\begin{aligned} \text{Cov}(x_{i,j(k)}, x_{i,l}) &= \mathbb{E}[f_{j(k)}(z_{ik})f_l(\mathbf{z}_i)] - \mathbb{E}[f_{j(k)}(z_{ik})]\mathbb{E}[f_l(\mathbf{z}_i)] \\ &= \frac{1}{c_{j'(k)}} \left[\mathbb{E}[f_{j'(k)}(z_{ik})f_l(\mathbf{z}_i)] - \mathbb{E}[f_{j'(k)}(z_{ik})]\mathbb{E}[f_l(\mathbf{z}_i)] \right] \\ &= \frac{1}{c_{j'(k)}} \text{Cov}(x_{i,j(k)}, x_{i,l}). \end{aligned}$$

As the rows of the covariance matrix (excluding diagonals) are parallel, then the rows $R_{j(k),\setminus j(k),j'(k)}, R_{j'(k),\setminus j(k),j'(k)}$ are also parallel.

Next, we assume $R_{l,\setminus\{l,p\}}$ and $R_{p,\setminus\{l,p\}}$ are parallel, and show that then l and p are anchor features for the same factor.

Then, there is a $c_{lp} \in \mathbb{R}$ such that for all $r \in \{1, \dots, G\} \setminus \{l, p\}$,

$$\begin{aligned} \text{Cov}(x_{i,l}, x_{i,r}) &= c_{lp} \text{Cov}(x_{i,p}, x_{i,r}) \\ \text{Cov}((f(\mathbf{z}_i)_l - c_{lp}f(\mathbf{z}_i)_p), x_{i,r}) &= 0. \end{aligned}$$

By [Assumption 3](#), then

$$f(\mathbf{z}_i)_l = c_{lp}f(\mathbf{z}_i)_p \quad \text{almost everywhere.}$$

By [Assumption 2](#), the only functions that are parallel are anchor features.

Consequently, using the arguments of [Bing et al. \(2023\)](#), we can detect the anchor features from the marginal population correlation matrix. The dimension of the latent space can also be identified from the number of sets of parallel rows. \square

Lemma 2. *The noise variances for anchor features are identifiable.*

Proof. For two anchor features $j(k), j'(k)$, for any non-anchor feature l , we have

$$\text{Cor}(x_{i,j(k)}, x_{i,l})/\text{Cor}(x_{i,j'(k)}, x_{i,l}) = c_{j'(k)},$$

so $c_{j'(k)}$ is identifiable. Then, for

$$\text{Cov}(x_{i,j(k)}, x_{i,j'(k)}) = c_{j'(k)} \text{Var}(f_{j(k)}(\mathbf{z}_i)),$$

so $\text{Var}(f_{j(k)}(\mathbf{z}_i))$ is identifiable. Consequently,

$$\sigma_{j(k)}^2 = \text{Var}(x_{i,j(k)}) - \text{Var}(f_{j(k)}(\mathbf{z}_i))$$

is identifiable. So, we have the noise variances corresponding to anchor features are identifiable. \square

Lemma 3. *Suppose we have two solutions $(f, \mathbf{W}, p_z, \Sigma)$, $(\hat{f}, \hat{\mathbf{W}}, p_{\hat{z}}, \hat{\Sigma})$ such that*

$$p(\mathbf{x}_i | \mathbf{W}, f, \Sigma) = p(\mathbf{x}_i | \hat{\mathbf{W}}, \hat{f}, \hat{\Sigma})$$

Then, under [Assumptions 1 to 3](#), we have $(z_1, \dots, z_K) \stackrel{d}{=} (h_1(\hat{z}_{\pi(1)}), \dots, h_K(\hat{z}_{\pi(K)}))$, where π is a permutation and $h_k : \mathbb{R} \rightarrow \mathbb{R}$ are invertible functions.

Proof. From [Lemma 1](#), we can identify the anchor features. This is up to permutation: suppose $x_{i,j(k)}$ is an anchor feature for factor dimension k . Then we have $w_{j(k),k} \neq 0$, $w_{j(k),k'} = 0$, $k' \neq k$. For the alternate solution, we have $\hat{w}_{j(k),\pi(k)} \neq 0$, $\hat{w}_{j(k),\pi(k')} = 0$, $k' \neq k$, for some permutation $\pi(k)$.

Denote:

$$\begin{aligned} \mathbf{S} &:= (f_{j(1)}(z_{i1}), \dots, f_{j(K)}(z_{iK})), \\ \hat{\mathbf{S}} &:= (\hat{f}_{j(1)}(\hat{z}_{i,\pi(1)}), \dots, \hat{f}_{j(K)}(\hat{z}_{i,\pi(K)})). \end{aligned}$$

We have:

$$\mathbf{S} + \boldsymbol{\varepsilon}_{i,\mathcal{A}} = \hat{\mathbf{S}} + \hat{\boldsymbol{\varepsilon}}_{i,\mathcal{A}}$$

where $\boldsymbol{\varepsilon}_{i,\mathcal{A}}, \hat{\boldsymbol{\varepsilon}}_{i,\mathcal{A}} \stackrel{\text{ind}}{\sim} N(0, \Sigma_{\mathcal{A}})$ and $\Sigma_{\mathcal{A}} = \text{diag}(\sigma_{j(1)}^2, \dots, \sigma_{j(K)}^2)$. From [Lemma 2](#), $\Sigma_{\mathcal{A}}$ is identifiable.

Because the characteristic function of a Gaussian is never zero, we can deconvolve the noise and obtain:

$$(f_{j(1)}(z_{i1}), \dots, f_{j(K)}(z_{iK})) \stackrel{d}{=} (\hat{f}_{j(1)}(\hat{z}_{i,\pi(1)}), \dots, \hat{f}_{j(K)}(\hat{z}_{i,\pi(K)})).$$

Define the vector map $H : \mathbb{R}^K \rightarrow \mathbb{R}^K$, $H(u_1, \dots, u_K) = (f_{j(1)}^{-1} \circ \hat{f}_{j(1)}(u_1), \dots, f_{j(K)}^{-1} \circ \hat{f}_{j(K)}(u_K))$. Define $h_k := f_{j(k)}^{-1} \circ \hat{f}_{j(k)}$.

Then, we have

$$(z_{i1}, \dots, z_{iK}) \stackrel{d}{=} (h_1(\hat{z}_{i,\pi(1)}), \dots, h_K(\hat{z}_{i,\pi(K)})).$$

□

Lemma 4. Suppose we have two solutions $(f, \mathbf{W}, p_z, \Sigma)$, $(\hat{f}, \hat{\mathbf{W}}, p_{\hat{z}}, \hat{\Sigma})$ such that

$$p(\mathbf{x}|\mathbf{W}, f, \Sigma) = p(\mathbf{x}|\hat{\mathbf{W}}, \hat{f}, \hat{\Sigma})$$

Then, with [Assumptions 1 to 5](#), the support of \mathbf{W} and $\hat{\mathbf{W}}$ is the same (up to permutation of columns).

Proof. We first show that we can obtain latent transformations u_1, \dots, u_K such that we have the same joint distribution $(x_1, \dots, x_G, u_1, \dots, u_K)$ across parameterizations (f, \mathbf{W}, p_z) , $(\hat{f}, \hat{\mathbf{W}}, p_{\hat{z}})$ which have the same marginal distribution on \mathbf{x} .

Consider an anchor feature $j(k)$ for factor dimension k :

$$x_{j(k)} = f_{j(k)}(z_k) + \varepsilon_{j(k)}$$

Because the distribution of $\varepsilon_{j(k)}$ is Gaussian with known variance ([Lemma 2](#)), and independent of z_k , we can identify the distribution of $f_{j(k)}(z_k)$, where $\mathbf{z} \sim p_z$ (e.g. see classic nonparametric deconvolution results, [Carroll and Hall \(1988\)](#)).

Now, define $v_k = f_{j(k)}(z_k)$. Then, define $u_k = F_{v_k}(v_k)$ where F_{v_k} is the CDF of v_k , so u_k is a strictly monotone function of v_k . We can repeat this for all anchor features to obtain $\mathbf{u} = (u_1, \dots, u_K)$.

The joint distribution (\mathbf{x}, \mathbf{u}) is well-defined because (\mathbf{x}, \mathbf{u}) is a measurable function of $(\mathbf{z}, \boldsymbol{\epsilon})$. Moreover, we can use the same construction for the alternative parameterization to obtain $(\mathbf{x}, \hat{\mathbf{u}}) \stackrel{d}{=} (\mathbf{x}, \mathbf{u})$.

We now argue by contradiction that \mathbf{W} and $\hat{\mathbf{W}}$ have the same support.

Suppose there exists an entry $(l, 1)$ such that $w_{l1} = 0$ but $\hat{w}_{l1} \neq 0$.

We can write:

$$x_l \stackrel{d}{=} g(u_2, \dots, u_K) + \varepsilon_l,$$

where $g(u_2, \dots, u_K) := f_l(0, w_{l2} f_{j(2)}^{-1}(F_{v_2}^{-1}(u_2)), \dots, w_{lK} f_{j(K)}^{-1}(F_{v_K}^{-1}(u_K)))$.

Note also:

$$x_l \stackrel{d}{=} \hat{g}(u_1, \dots, u_K) + \varepsilon_l,$$

where $\hat{g}(u_1, \dots, u_K) := \hat{f}_l(\hat{w}_{l1} \hat{f}_{j(1)}^{-1}(F_{v_1}^{-1}(u_1)), \dots, \hat{w}_{lK} \hat{f}_{j(K)}^{-1}(F_{v_K}^{-1}(u_K)))$.

We consider the conditional variance of x_l given $\mathbf{u}_{\setminus 1} = (u_2, \dots, u_K)$.

The conditional variance is:

$$\text{Var}(x_l | \mathbf{u}_{\setminus 1}) = 0 + \sigma_l^2.$$

Now consider the conditional variance from the alternative parameterization with $\hat{w}_{l1} \neq 0$:

$$\text{Var}(x_l | \mathbf{u}_{\setminus 1}) = \text{Var}(\hat{g}(\mathbf{u} | \mathbf{u}_{\setminus 1})) + \hat{\sigma}_l^2.$$

When $\hat{w}_{lk} \neq 0$, this conditional variance is not constant almost everywhere in $\mathbf{u}_{\setminus 1}$, because of the non-degeneracy [Assumptions 4](#) and [5](#). (Note the non-degeneracy of $p_z(z_1 | \mathbf{z}_{\setminus 1})$ means that $p_u(u_1 | \mathbf{u}_{\setminus 1})$ is also non-degenerate, as u_1 is a strictly monotone function of z_1).

This contradicts the distributional equality. So, $\hat{w}_{l1} = 0$.

We repeat this argument for all $l = 1, \dots, G$, $k = 1, \dots, K$. Consequently, we must have $\text{supp}(\mathbf{W}) \subseteq \text{supp}(\widehat{\mathbf{W}})$. We can make the same argument in reverse to obtain $\text{supp}(\widehat{\mathbf{W}}) \subseteq \text{supp}(\mathbf{W})$. \square

Lemma 5. *The noise variances Σ are identifiable.*

Proof. We need to prove that the noise variance of the non-anchor features are identifiable.

Consider again (\mathbf{x}, \mathbf{u}) as defined in the proof of [Lemma 4](#). We have

$$\mathbb{E}[x_l | u_1, \dots, u_K] = g_l(u_1, \dots, u_K),$$

where $g(u_1, \dots, u_K) := f_l(w_{l1} f_{j(1)}^{-1}(F_{v_1}^{-1}(u_1)), \dots, w_{lK} f_{j(K)}^{-1}(F_{v_K}^{-1}(u_K)))$.

We also have

$$\mathbb{E}[x_l | u_1, \dots, u_K] = \hat{g}_l(u_1, \dots, u_K),$$

where $\hat{g}(u_1, \dots, u_K) := \hat{f}_l(\hat{w}_{l1} \hat{f}_{j(1)}^{-1}(F_{v_1}^{-1}(u_1)), \dots, \hat{w}_{lK} \hat{f}_{j(K)}^{-1}(F_{v_K}^{-1}(u_K)))$.

Consequently,

$$g_l(u_1, \dots, u_K) = \hat{g}_l(u_1, \dots, u_K) \quad \text{almost everywhere.} \quad (\text{A.1})$$

Now,

$$\begin{aligned} \text{Var}(x_l) &= \text{Var}(\mathbb{E}[x_l|u_1, \dots, u_K]) + \mathbb{E}[\text{Var}(x_l|u_1, \dots, u_K)] \\ &= \sigma_l^2 + \text{Var}(g_l(u_1, \dots, u_K)) \\ &= \sigma_l^2 + \text{Var}(\hat{g}_l(u_1, \dots, u_K)) \quad (\text{Eq. A.1}) \\ &= \hat{\sigma}_l^2 + \text{Var}(\hat{g}_l(u_1, \dots, u_K)) \quad (\text{equality of distributions}). \end{aligned}$$

Hence, $\sigma_l^2 = \hat{\sigma}_l^2$.

□

Theorem 1. *Suppose Assumptions 1 to 5 hold. Then*

1. *The anchor features and the latent dimensionality K are identifiable from the marginal population correlation matrix.*
2. *For any two solutions $(f, \mathbf{W}, \Sigma, p_z)$, $(\hat{f}, \hat{\mathbf{W}}, \hat{\Sigma}, \hat{p}_z)$ with*

$$p(\mathbf{x}_i|f, \mathbf{W}, \Sigma) = p(\mathbf{x}_i|\hat{f}, \hat{\mathbf{W}}, \hat{\Sigma}),$$

the factors are equal in distribution up to element-wise transformations and permutations:

$$(z_{i1}, \dots, z_{iK}) \stackrel{d}{=} (h_1(\hat{z}_{i,\pi(1)}), \dots, h_K(\hat{z}_{i,\pi(K)})),$$

where $h_k : \mathbb{R} \rightarrow \mathbb{R}$ are invertible functions and $\pi : \{1, \dots, K\} \rightarrow \{1, \dots, K\}$ is a permutation.

3. *The support of \mathbf{W} is identifiable, up to permutation of columns.*
4. *The error variances Σ are identifiable.*

Proof. Combining Lemmas 1 to 5, the theorem is proved. □

Theorem 2. *Suppose Assumptions 1 to 5 hold for each study, considered separately. Then, the supports of the shared matrix $\mathbf{W}^{(S)}$ and study-specific matrices $\mathbf{W}^{(m)}$ are identifiable.*

Proof. First, we consider each study separately. From Theorem 1, for each study m , we can identify the support of $[\mathbf{W}^{(S)}, \mathbf{W}^{(m)}]$ up to column permutation. (Note: column permutation means that the shared and study-specific columns cannot be partitioned).

Second, we consider all studies and extract the columns of $\{[\mathbf{W}^{(S)}, \mathbf{W}^{(m)}]\}_{m=1}^M$ which have the same support across all studies. These columns form $\mathbf{W}^{(S)}$.

Finally, the remaining columns for each study are the study-specific columns $\mathbf{W}^{(m)}$. By construction, these columns did not match across all studies (otherwise they would be in $\mathbf{W}^{(S)}$). Because of the anchor feature structure, the columns $\{\mathbf{W}^{(m)}\}_{m=1}^M$ have disjoint supports on the anchor indices, and so the intersection of their column spaces is null (i.e. they do not have shared signal remaining). \square

B Implementation details

B.1 Architecture

For the encoders, we use two-layer ReLU feed forward neural networks with batch norm:

$$\begin{aligned}\mathbf{h}_\psi^{(1)}(\mathbf{x}_i) &= \text{ReLU}(\text{BN}_\psi^{(1)}(\mathbf{V}_\psi^{(1)}\mathbf{x}_i + \mathbf{b}_\psi^{(1)})) \\ \mathbf{h}_\psi^{(2)}(\mathbf{x}_i) &= \text{ReLU}(\text{BN}_\psi^{(2)}(\mathbf{V}_\psi^{(2)}\mathbf{h}_\psi^{(1)}(\mathbf{x}_i) + \mathbf{b}_\psi^{(2)})) \\ \mu_\psi(\mathbf{x}_i) &= \mathbf{V}_\psi^{(\mu)}\mathbf{h}_\psi^{(2)}(\mathbf{x}_i) + \mathbf{b}_\psi^{(\mu)} \\ \sigma_\psi(\mathbf{x}_i) &= \mathbf{V}_\psi^{(\sigma)}\mathbf{h}_\psi^{(2)}(\mathbf{x}_i) + \mathbf{b}_\psi^{(\sigma)},\end{aligned}$$

where $\mathbf{V}_\psi^{(l)} \in \mathbb{R}^{d_{\text{out}} \times d_{\text{in}}}$ is the weight matrix for layer l with input dimension d_{in} and output dimension d_{out} , and $\mathbf{b}_\psi^{(l)} \in \mathbb{R}^{d_{\text{out}}}$ is the bias/intercept vector for layer l . Further, $\text{BN}^{(l)}$ denotes standard batch norm (Ioffe and Szegedy, 2015) and $\text{ReLU}(z) = \max\{0, z\}$.

For the decoder, we use a two-layer ReLU feed forward neural network with a skip connection from the masked latents to the output dimension. Specifically, for the output dimension j of sample i from study m , denote the masked latents as $\mathbf{c}_{ij}^{(m)} = \widetilde{\mathbf{w}}_j^{(m)} \odot \widetilde{\mathbf{z}}_i^{(m)}$. Then,

$$\begin{aligned}\mathbf{h}_\theta^{(1)}(\mathbf{c}_{ij}^{(m)}) &= \text{ReLU}(\mathbf{V}_\theta^{(1)}(\mathbf{c}_{ij}^{(m)})) \\ \mathbf{h}_\theta^{(2)}(\mathbf{c}_{ij}^{(m)}) &= \text{ReLU}(\mathbf{V}_\theta^{(2)}\mathbf{h}_\theta^{(1)}(\mathbf{c}_{ij}^{(m)}) + \mathbf{b}_\theta^{(2)}) \\ f_j(\mathbf{c}_{ij}^{(m)}) &= \begin{cases} (\mathbf{v}_{\theta,j}^{(3)})^\top [\mathbf{h}_\theta^{(2)}(\mathbf{c}_{ij}^{(m)}) + \mathbf{c}_{ij}^{(m)}] + b_{\theta,j}^{(3)} & \text{(Gaussian MSSVAE)} \\ \text{softplus}[(\mathbf{v}_{\theta,j}^{(3)})^\top [\mathbf{h}_\theta^{(2)}(\mathbf{c}_{ij}^{(m)}) + \mathbf{c}_{ij}^{(m)}] + b_{\theta,j}^{(3)}] & \text{(NB-MSSVAE)} \end{cases}\end{aligned}$$

where $\mathbf{v}_{\theta,j}^\top$ is the j th row of $\mathbf{V}_\theta^{(3)}$. That is, each of the G outputs of f share all neural network parameters until the final layer.

The dimensions of the hidden layers used for experiments are given in [Table 2](#).

B.2 Optimization

The objective function is:

$$\begin{aligned} \mathcal{L}(\Theta) = & \sum_{m=1}^M \left\{ \sum_{i=1}^{n_m} \left\{ \mathbb{E}_{q_{\psi_S}(\mathbf{z}_i^{(m)}|\mathbf{x}_i^{(m)})q_{\psi_m}(\boldsymbol{\zeta}_i^{(m)}|\mathbf{x}_i^{(m)})} \left[\log p_{\theta}(\mathbf{x}_i^{(m)}|\mathbf{W}^{(S)}, \mathbf{W}^{(m)}, \mathbf{z}_i^{(m)}, \boldsymbol{\zeta}_i^{(m)}, \boldsymbol{\Sigma}) \right] \right. \right. \\ & - D_{KL}(q_{\psi_S}(\mathbf{z}_i^{(m)}|\mathbf{x}_i^{(m)})||p(\mathbf{z}_i^{(m)})) - D_{KL}(q_{\psi_m}(\boldsymbol{\zeta}_i^{(m)}|\mathbf{x}_i^{(m)})||p(\boldsymbol{\zeta}_i^{(m)})) \} \\ & + \mathbb{E}_{\boldsymbol{\Gamma}^{(m)}|\mathbf{W}^{(m)}, \boldsymbol{\eta}^{(m)}} [\log p(\mathbf{W}^{(m)}|\boldsymbol{\Gamma}^{(m)})p(\boldsymbol{\Gamma}^{(m)}|\boldsymbol{\eta}^{(m)})p(\boldsymbol{\eta}^{(m)})] \} \\ & \left. \left. + \mathbb{E}_{\boldsymbol{\Gamma}^{(S)}|\mathbf{W}^{(S)}, \boldsymbol{\eta}^{(S)}} [\log p(\mathbf{W}^{(S)}|\boldsymbol{\Gamma}^{(S)})p(\boldsymbol{\Gamma}^{(S)}|\boldsymbol{\eta}^{(S)})p(\boldsymbol{\eta}^{(S)})] + \log p(\boldsymbol{\Sigma}) \right. \right\} \end{aligned} \quad (\text{B.1})$$

We optimize [Eq. B.1](#) by alternating between an expectation step and a maximization step.

B.2.1 Expectation step

To approximate the first term of [Eq. B.1](#), we use Monte Carlo. When the likelihood is Gaussian, this corresponds to:

$$\mathbb{E}_{q_{\psi_S}(\mathbf{z}_i^{(m)}|\mathbf{x}_i^{(m)})q_{\psi_m}(\boldsymbol{\zeta}_i^{(m)}|\mathbf{x}_i^{(m)})} \left[\log p_{\theta}(\mathbf{x}_i^{(m)}|\mathbf{W}^{(S)}, \mathbf{W}^{(m)}, \mathbf{z}_i^{(m)}, \boldsymbol{\zeta}_i^{(m)}, \boldsymbol{\Sigma}) \right] \quad (\text{B.2})$$

$$\approx \frac{1}{L} \sum_{l=1}^L \sum_{j=1}^G \frac{1}{\sigma_j^2} \left[x_{ij} - f_j(\tilde{\mathbf{w}}_j^{(m)} \odot \tilde{\mathbf{z}}_i^{(m), (l)}) \right]^2, \quad (\text{B.3})$$

where we draw the samples $\tilde{\mathbf{z}}_i^{(m), (l)}$ as

$$\tilde{\mathbf{z}}_i^{(m), (l)} = \left(\mathbf{z}_i^{(m), (l)} \quad \mathbf{0}_{1 \times (K_S + K_1 + \dots + K_{m-1})} \quad \boldsymbol{\zeta}_i^{(m), (l)} \quad \mathbf{0}_{1 \times (K_{m+1} + \dots + K_M)} \right)$$

with

$$\begin{aligned} \mathbf{z}_i^{(m), (l)} &= \mu_{\psi_S}(\mathbf{x}_i) + \sigma_{\psi_S}(\mathbf{x}_i) \odot \boldsymbol{\xi}_i^{(m), (l)}, \quad \boldsymbol{\xi}_i^{(m), (l)} \sim N(\mathbf{0}, \mathbf{I}), \\ \boldsymbol{\zeta}_i^{(m), (l)} &= \mu_{\psi_m}(\mathbf{x}_i) + \sigma_{\psi_m}(\mathbf{x}_i) \odot \boldsymbol{\nu}_i^{(m), (l)}, \quad \boldsymbol{\nu}_i^{(m), (l)} \sim N(\mathbf{0}, \mathbf{I}). \end{aligned}$$

That is, we draw standard Gaussian random variables and then obtain samples from the variational posterior by multiplying by standard deviation and adding the mean. For the NB-MSSVAE, the process is the same, replacing [Eq. B.3](#) with the negative-binomial log likelihood.

For the remaining terms, the calculations are the same for the shared and study-specific parameters, so we write the general formula, omitting the superscripts.

The KL divergence between the variational posterior $q_{\psi}(\mathbf{z}_i|\mathbf{x}_i)$ and the prior $\mathbf{z}_i \sim N(\mathbf{0}, \mathbf{I})$ is:

$$D_{KL}(q_{\psi}(\mathbf{z}_i|\mathbf{x}_i)||p(\mathbf{z}_i)) = \frac{1}{2} \sum_{k=1}^K \left[1 + \log(\sigma_{\psi}^2(\mathbf{x}_i) - (\mu_{\psi}(\mathbf{x}_i))^2 - \sigma_{\psi}^2(\mathbf{x}_i)) \right].$$

For the spike-and-slab lasso prior terms, we have:

$$\begin{aligned} \mathbb{E}_{\boldsymbol{\Gamma}|\boldsymbol{W}^{\text{old}}, \boldsymbol{\eta}^{\text{old}}} [\log p(\boldsymbol{W}|\boldsymbol{\Gamma})p(\boldsymbol{\Gamma}|\boldsymbol{\eta})p(\boldsymbol{\eta})] &= \sum_{k=1}^K \sum_{j=1}^G \lambda^*(w_{jk}^{\text{old}}, \eta_k^{\text{old}}) |w_{jk}| \\ &\quad + \sum_{k=1}^K \left[\sum_{j=1}^G \mathbb{E}[\gamma_{jk}|w_{jk}^{\text{old}}, \eta_k^{\text{old}}] + a - 1 \right] \log \eta_k \\ &\quad + \left[G - \sum_{j=1}^G \mathbb{E}[\gamma_{jk}|w_{jk}^{\text{old}}, \eta_k^{\text{old}}] + b - 1 \right] \log(1 - \eta_k), \end{aligned}$$

where

$$\begin{aligned} \mathbb{E}[\gamma_{jk}|w_{jk}, \eta_k] &= \frac{\eta_k \lambda_1 \exp(-\lambda_1 |w_{jk}|)}{\eta_k \lambda_1 \exp(-\lambda_1 |w_{jk}|) + (1 - \eta_k) \lambda_0 \exp(-\lambda_0 |w_{jk}|)} \\ \lambda^*(w_{jk}, \eta_k) &= \lambda_1 \mathbb{E}[\gamma_{jk}|w_{jk}, \eta_k] + \lambda_0 (1 - \mathbb{E}[\gamma_{jk}|w_{jk}, \eta_k]). \end{aligned}$$

B.2.2 Maximization step

In the maximization step, we take a gradient step over parameters Θ . The derivatives of $L(\Theta)$ are calculated using automatic differentiation.

B.2.3 Stochastic optimization

In experiments, we use stochastic optimization. At each epoch, we split our data into mini-batches. For each mini-batch, we evaluate the expectations and take a gradient step. For the gradient steps, we use Adam (Kingma and Ba, 2015) with the default PyTorch parameters ($\beta_1 = 0.9, \beta_2 = 0.999$).

The mini-batches are selected using PyTorch's `WeightedRandomSampler` with each sample assigned a weight inversely proportional to the size of its associated group. This ensures each mini-batch has an approximately equal number of samples from each group.

C Empirical study details

C.1 Metrics

In this section, we provide more details about the metrics used for evaluation in the simulation studies.

The consensus (Hochreiter et al., 2010), and relevance and recovery scores (Prelić et al., 2006) are all based on the Jaccard index, a measure of similarity between two sets A and B :

$$J(A, B) = \frac{|A \cap B|}{|A \cup B|}. \quad (\text{C.1})$$

The Jaccard index penalizes estimates $\widehat{\mathbf{W}}$ which overestimate the support of the true \mathbf{W} .

Denote C_k as the set non-zero entries of the k th column $\mathbf{W}_{\cdot,k}$. Let $\mathcal{C}_t = \{C_1, \dots, C_K\}$ and let $\mathcal{C}_f = \{\widehat{C}_1, \dots, \widehat{C}_{\widehat{K}}\}$, where \widehat{C}_k is the set of non-zero entries of an estimated column $\widehat{\mathbf{W}}_{\cdot,k}$ and \widehat{K} is the estimated factor dimension. Then:

$$\text{Relevance} = \frac{1}{|\mathcal{C}_f|} \sum_{\widehat{C}_{k'} \in \mathcal{C}_f} \max_{C_k \in \mathcal{C}_t} J(C_k, \widehat{C}_{k'}), \quad (\text{C.2})$$

$$\text{Recovery} = \frac{1}{|\mathcal{C}_t|} \sum_{C_k \in \mathcal{C}_t} \max_{\widehat{C}_{k'} \in \mathcal{C}_f} J(C_k, \widehat{C}_{k'}), \quad (\text{C.3})$$

$$\text{Consensus} = \frac{1}{\max\{|\mathcal{C}_t|, |\mathcal{C}_f|\}} \sum_{C_k \in \mathcal{C}_t} J(C_k, \widehat{C}_{\pi(k)}), \quad (\text{C.4})$$

where π is the optimal assignment of the estimated $\widehat{C}_{k'}$ to the true C_k (based on Jaccard scores), calculated using the Hungarian algorithm (Munkres, 1957).

The disentanglement score of Eastwood and Williams (2018) measures how important each estimated factor dimension $\widehat{\mathbf{z}}_{\cdot k'}$ is for a particular true factor dimension $\mathbf{z}_{\cdot k}$, penalizing estimated factors which are predictive of multiple true factor dimensions. The disentanglement score is calculated as follows.

1. For each true factor dimension k , train a gradient boosted tree to predict z_{ik} from $\widehat{\mathbf{z}}_i$.
2. Record the importance of each $\widehat{z}_{ik'}$ for predicting z_{ik} as $R_{k',k}$ (these are the importance scores from the gradient boosted tree).
3. Calculate the score of $\widehat{\mathbf{z}}_{\cdot k'}$ as:

$$D(\widehat{\mathbf{z}}_{\cdot k'}) = 1 - H_K(P_{k' \cdot})$$

where $H_K(P_{k' \cdot}) = -\sum_{k=1}^K P_{k',k} \log_K(P_{k',k})$ is the entropy and $P_{k',k} = R_{k',k} / \sum_{k=1}^K R_{k',k}$ denotes the weighted importance of $\widehat{z}_{ik'}$ for predicting z_{ik} . If $\widehat{z}_{ik'}$ is important for predicting a single factor dimension, the score is 1. If \widehat{z}_{ik} is equally important for all factor dimensions, the score is zero.

4. The overall disentanglement score is the weighted sum:

$$D(\widehat{\mathbf{z}}) = \sum_{k'=1}^{\widehat{K}} \rho_{k'} D(\widehat{\mathbf{z}}_{\cdot k'}) \quad (\text{C.5})$$

where $\rho_{k'} = \sum_{k=1}^K R_{k',k} / \sum_{k,k'=1}^{\widehat{K}} R_{k',k}$. If $\widehat{z}_{k'}$ is irrelevant for every $\{z_k\}_{k=1}^K$, then $\rho_{k'} \approx 0$ and $\widehat{z}_{k'}$ does not contribute to the disentanglement score.

C.2 Experiment settings

C.2.1 Hyperparameter settings

[Table 2](#) displays the fixed hyperparameter settings for each experiment.

Table 2: Hyperparameter settings for experiments.

Hyperparameter	Gaussian	Synthetic RNA	Platelet
Batch Size	512	512	512
Epochs	500	800	800
Hidden Dimensions	[50, 50]	[256, 128]	[256, 128]
Initial K_S	30	50	50
Initial K_m	5	10	10
Learning Rate (not W)	0.01	0.001	0.001
Learning Rate (W)	0.01	0.01	0.01

Spike-and-slab lasso parameters. For the regularization parameters, we set $\lambda_1 = 0.1$. For λ_0 , we adopt an annealing strategy. Specifically, for the first 5% of epochs, $\lambda_0 = 1$. For the next 25% of epochs, $\lambda_0 = 10$. For the remaining epochs, $\lambda_0 = 15$.

For all experiments, the MSSVAE takes the η_k prior hyperparameters to be $a = 1, b = G$, where G is the number of observed features.

Noise parameter settings. For the Gaussian MSSVAE, the prior on the noise variance is

$$\sigma_j^2 \sim \text{Inverse-Gamma}(\alpha, \beta). \quad (\text{C.6})$$

Following [Moran et al. \(2022\)](#), we set $\alpha = 1.5$. The hyperparameter β is set to a data-dependent value. Specifically, we first calculate the sample variance of each feature, $\mathbf{x}_{\cdot j}$. Then, we set β such that the 5% quantile of the sample variances is the 90% quantile of the Inverse-Gamma prior.

C.2.2 Parameter initializations

Noise parameter initializations. For the Gaussian MSSVAE, the variance σ^2 is set to the 0.05-quantile of the empirical variance of each of the G columns ([Moran et al., 2022](#)).

For the NB-MSSVAE, the inverse dispersion ϕ_g is initialized based on a moment estimator:

$$\phi_g^{(\text{init})} = \frac{\hat{\mu}_g}{\hat{\sigma}_g^2 - \hat{\mu}_g},$$

where $\hat{\mu}_g$ and $\hat{\sigma}_g^2$ are the empirical mean and variance, respectively, of gene g .

W initialization. We initialize the entries of $\mathbf{W}^{(S)}$ and $\mathbf{W}^{(m)}$ to 1.

Neural network parameters. We use the default PyTorch initialization.

C.3 Additional results

Here we show the worst performing replicate in the Gaussian nonlinear factor analysis setting (§ 4.1).

Figure 6 shows the estimated masking matrices for this data replicate; one of the shared blocks has instead been estimated as part of each of the study-specific blocks. This could be resolved through post-processing.

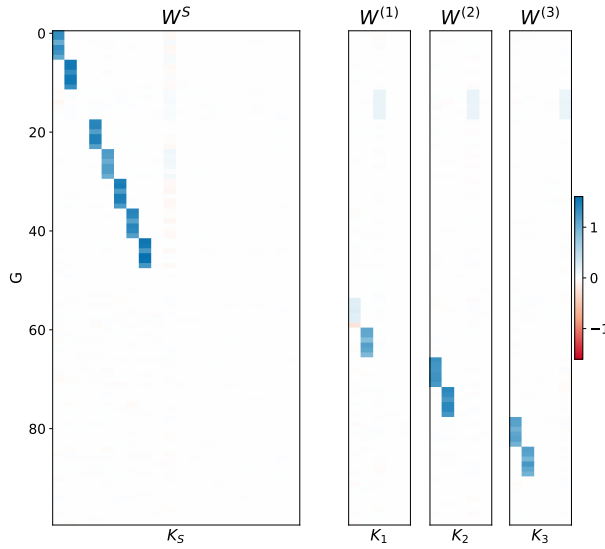


Figure 6: Gaussian nonlinear factor analysis: worst performing MSSVAE experiment in terms of average consensus score.

C.4 Platelet data processing

We process the platelet RNA-sequencing data as follows.

- Remove samples with total number of transcripts less than $e^{12.5}$;
- Keep only genes that had at least 25 counts over all samples;
- Keep only genes with counts-per-million greater than 1 for at least 20% of samples;
- Keep the top 5000 most variable genes based on Pearson residuals of a negative binomial offset model (Lause et al., 2021), implemented using scanpy (Wolf et al., 2018).